

BEAM BREAK-UP EXPERIMENTS AT SLAC[†]

O. H. Altenmueller, E. V. Farinholt, Z. D. Farkas, W. B. Herrmannsfeldt, H. A. Hogg,
 R. F. Koontz, C. J. Kruse, G. A. Loew, and R. H. Miller

Stanford Linear Accelerator Center
 Stanford University, Stanford, California

Introduction

The first observation of beam break-up at SLAC was made on April 27, 1966, one week after the beam was first turned on over two-thirds of the accelerator's two-mile length.¹ The event caused more astonishment than panic because the observed beam break-up current threshold of 10 to 20 mA peak, while much lower than in other shorter accelerators, was not far from the 50 mA peak current specified for the two-mile accelerator.

During the past five months, considerable analytical and experimental work has been done at SLAC to understand the beam break-up effect and to formulate a practical corrective program. Two papers are being presented at this conference on this work. One of them, by R.H. Helm,² summarizes most of the theoretical and analytical work. In turn, the present paper attempts to describe most of the experiments carried out, both on cold tests and on the accelerator itself. In addition to the authors of this paper, a large number of staff members at SLAC participated in the experiments and contributed to specific suggestions and discussions. In summary, this paper will start out by describing the beam break-up effect, both qualitatively and quantitatively, as it has been observed and understood so far. This description will be followed by the presentation of results derived from microwave cold tests, microwave beam tests, focusing beam tests, and a few other miscellaneous experiments involving the beam. From all these experiments, it will be seen how the presently adopted corrective program was arrived at. A short description of the remedies will be given, together with the improvements to be expected.

Qualitative and Quantitative Description of Beam Break-up

The basic manifestation of the beam break-up effect at SLAC is illustrated in Fig. 1. As can be seen from the three video pulses, the beam pulse length, specified at about 1.6 μsec, is shortened erratically when the beam current is increased above a certain value. The shortening becomes more pronounced as the current from the injector is increased. The pattern of pulses* shown in Fig. 1 can be observed at any location along the accelerator and the onset of break-up is determined by the beam current transmitted through that point. Figure 2 shows an example of two different beam profiles along the machine. The ordinate of each dot represents the amount of charge transmitted past the

end of a given sector of the accelerator. In the upper photograph, the beam current from the injector is at a level below the beam break-up threshold for the particular energy and pulse length shown, and, except for slight undulations due to imperfect amplifier calibration and noise, no current is lost along the 30 sectors of the machine. In the lower photograph, the current from the injector has been increased to a level far above break-up and it is seen that beyond sector 12, an increasingly large fraction of the electrons are lost through scraping by the accelerator and collimator walls. The electrons transmitted beyond sector 12 correspond to increasingly earlier parts of the injector pulse. Presumably, if the machine were infinitely long, no electron bunches would reach the end. A similar illustration of this effect is shown in Fig. 3. This figure is a profile of the pulse obtained from PLIC, Panofsky's Long Ion Chamber. This two-mile long argon-filled coaxial line installed in the accelerator housing breaks down under the effect of ionization caused by the lost electrons and the resulting transmitted pulse yields a profile of lost beam power along the machine. The peaks on the fine structure of the PLIC display correspond to maximum ionization caused by scraping by the collimators at the end of each of the 30 sectors. Their I.D. is 1.7 cm, two millimeters less than the smallest accelerator iris. Here also, beam break-up starts at sector 12 and there are 18 peaks to the end of the machine. Much of the quantitative data presented in this paper have been derived from displays of which these first three figures are typical examples.

In addition, various other types of equipment have been used in the beam break-up experiments. Most of them are schematically illustrated in Fig. 4. Because of the lack of available space and the need to operate some of the devices under vacuum, installation of this equipment was somewhat restricted and inflexible. The individual devices will be described later in this paper. Much of the experimental work was performed at the end of sector 19 where the beam could be momentum-analyzed and stopped, while installation work in the switchyard was proceeding. The beam break-up stimulation experiments were performed using accelerator section 1-C, shown downstream of the injector (after the corresponding klystron had been removed), and the special cavities around the 40-foot point. Experiments involving the entire length of the machine made use of the Cerenkov profile monitors in the beam switchyard.

Since the mathematical formulation of the beam break-up effect is given in detailed form in the theoretical paper by R. Helm,² no attempt will be made here to include an analytic description of the mechanism. However, a few basic facts pertinent to the model will be enumerated below.

* It should be mentioned that the rise time of these pulses is in reality much sharper than shown. The slight degradation in pulse shape is due to the response of the toroid and not to the shape of the injector pulse.

[†] Work supported by U. S. Atomic Energy Commission.

(Presented at 1966 Linear Accelerator Conference, Los Alamos, October 1966)

(a) As reported in the past by other authors, the beam break-up effect is due to the excitation by the electron beam of the TM_{11} -like deflecting mode, sometimes called the HEM_{11} mode. However, in contrast to the regenerative type of break-up observed in short accelerators, the growth of the mode and the deflection of the beam in this accelerator are the result of a cumulative multi-section interaction.

(b) A small transverse modulation of the electron bunches at the beginning of the accelerator excites the mode, which in turn, reacts on the next bunches. These undergo further modulation and in turn feed more energy into the mode. Thus, the effect is coherent within each beam pulse and cumulative both as a function of time and length. As the accelerator current is increased above the beam break-up threshold, the effect at first appears in the vertical direction. At higher currents, however, the orientation of the break-up plane becomes isotropic and random from pulse to pulse.

(c) The frequency at which the TM_{11} mode gets excited, at least predominantly, is approximately 4140 MHz. As illustrated in Fig. 5, the 4140 MHz wave produces a force on the electron bunches which are spaced at time intervals inversely proportional to the accelerating frequency, 2856 MHz. Because of the difference in wavelength, the electron bunches receive varying amounts of transverse momentum. As they move along the accelerator and receive increasingly large impulses, the growing sine wave representing the envelope of their displacement appears at 4140 MHz as well as at the difference frequency, 4140 - 2856 = 1284 MHz, as illustrated at the bottom of Fig. 5. In addition, it is also observed that similar envelopes can be drawn at other frequencies, such as the difference between the third harmonic of 2856 minus 4140, i.e. 4428 MHz. Similarly, one also obtains an envelope at 4428 - 2856 = 1572 MHz. It is important to understand that while the microwave interaction and amplification process takes place only at 4140 MHz, the other frequencies are always present in the transverse modulation. Not only can they be detected on the electron beam but it is also possible to perform microwave experiments at these frequencies. As discussed below, the fact that this is possible conveniently widens the choice of frequencies for these experiments.

(d) While the initial transverse modulation probably arises through noise or shock excitation, it is possible to precipitate and sharpen the effect by artificially stimulating the beam early in the machine by means of a small amount of rf power at any one of the above frequencies. The effect of this stimulation is illustrated in Fig. 6. Notice that whereas natural beam break-up at 10.1 mA is somewhat erratic, stimulated beam break-up is sharp and stable.

(e) For maximum amplification of the TM_{11} mode, it can be shown that there is a 45° difference between the phase of maximum transverse momentum and the phase of maximum displacement. This value of 45° is reached asymptotically with phase modulation occurring during the build-up time. However, because of the short time available during each beam pulse (1.6 μsec maximum) and the incoherence from pulse to pulse, it has not been possible to measure this phase modulation.

The analytic expressions and computer programs² which predict the beam break-up threshold as a function of time, distance, current and energy have been tested experimentally under a variety of conditions. In

particular, several experiments were performed to verify the predictions of the simple asymptotic expression for the transverse modulation, in the absence of focusing, given by

$$y = y_0 \exp \left[\left(K \frac{r_T}{Q} \frac{l_1}{L} \frac{tiz}{\frac{dy}{dz}} \right)^{1/3} - \frac{\omega t}{2Q} \right]$$

where t is the time to break-up, i is the current, z is the distance to break-up, r_T is the transverse shunt impedance, Q is the loss-factor, l_1 is the interaction length, L is the distance between interaction regions, K is a constant and $d\gamma/dz$ is the energy gradient. This expression applies in the case of uniform acceleration. Another slightly more complicated formula has been derived for the case where the beam is accelerated up to a given energy and then coasts along the rest of the machine.

The next few figures summarize the quantitative data obtained under weak focusing conditions. Notice that the above expression gives the onset of break-up when y becomes equal to the radius of the accelerator aperture. Assuming a constant value of y_0 , this onset can occur for any combination of parameters leading to a constant exponent (found to be of the order of 22). As predicted by the formula, Figures 7 and 8 show that beam break-up current is a linear function of inverse distance. A straight line is also obtained in Fig. 9, where the beam break-up current is plotted as a function of energy for a constant distance of 30 sectors. Notice that the focusing along the accelerator, obtained by means of quadrupole doublets located at the end of each sector, was adjusted in each case to preserve a constant betatron wavelength of approximately 15 sectors. In contrast with these results, it has been found that for a given fixed setting of the quadrupole currents along the machine, simultaneous beams of different energies (obtained through equal acceleration at the beginning of the accelerator but different coasting distances downstream), all seem to break up at the same time and distance. This result indicates that a compensation takes place between focusing and energy. Fig. 10 summarizes these data. The points plotted here give the time to break-up, t , as a function of $(tiz)^{1/3}$. Identical points were obtained for beams of 5, 10.1 and 15.5 GeV. The three different curves correspond to break-up at three different points along the machine and hence to three different focusing conditions. If the above expression for y were rigorous and took into account focusing, these curves would also be straight lines.

Figure 11 is a plot of the transverse displacement modulation due to beam break-up as a function of the quantity $(iz)^{1/3}$. Notice that the amplitude y is plotted down to 10^{-3} cm. These data obviously were not measured directly but were obtained by correlating the results shown by the numbered points (which correspond to the onset of beam scraping by the accelerator) with the microwave power level induced in a cavity resonant at 4140 MHz at the end of sector 5. The circled points were obtained by deducing the y -amplitudes from smaller measured induced power levels. The best fit to the data is given in the figure.

Microwave Cold Tests

One of the important characteristics of the SLAC accelerating structure is that it is of the constant-gradient design.³ For the sake of completeness, Table 1, included herewith, gives the dimensions of each of the 86 accelerator cavities. Studies of the beam break-up effect indicate, however, that the build-up of the TM_{11} mode, at least at the current levels used so far in the machine (100 mA maximum), occurs only in the first 8 to 10 cavities of each ten-foot accelerator section. This fact is illustrated in Fig. 12, where a typical SLAC microwave specialist indicates the approximate length of interaction. Figure 13 shows in detail the ω - β or Brillouin diagrams for the TM_{11} mode measured with resonant cavity stacks corresponding to 3 locations (input, middle, and output) in the constant-gradient section. It has been found, both theoretically and experimentally, that because of the tapered nature of the constant-gradient design, there are discrete frequencies at which resonances over a number of cavities take place. The lowest resonant frequency found at the input of the accelerator is 4139.6 MHz. The phase shift of the first cavity beyond the coupler cavity at this frequency is 0.765π . Notice that as the wave travels down the accelerator, the phase shift per cavity at this frequency approaches π . The first observed resonance occurs when the total phase shift through the first 8 to 10 cavities adds up to a multiple of π . Notice also that this frequency is neither the frequency at the lowest π mode nor the frequency of interception of the $v_p = c$ line with the lowest ω - β diagram. Figure 14 shows a plot of the electric field intensity for this first resonance. The plot was obtained by exciting a 10-foot section through the accelerator coupler at 4139.6 MHz and by performing a perturbation measurement with a small bead, slightly off-axis. Notice that some of the field also leaks out backwards, through the accelerator cut-off hole. Figure 15 is a plot of the VSWR looking into the input of a 10-foot accelerator section as a function of frequency. At least the first three valleys agree closely with theoretical predictions.² It is assumed that if the beam current were increased sufficiently beyond the present values, the higher resonances would also be excited and amplified and thereby would cause further beam break-up at these higher frequencies. However, it appears that these resonances have increasingly lower amplitudes and, therefore, will probably not cause serious difficulties below 100 mA or so.

Figure 16 gives the passband of the 10-foot constant-gradient section taken as a whole. As seen, this passband is only about 15 MHz wide. So far, frequencies within this band have not been measured on the beam. This is understandable from the fact that they correspond to waves totally asynchronous with the electrons so interaction is not cumulative.

One of the key experimental observations which has not been discussed in detail so far is that the beam break-up effect seems to occur first in the vertical direction. It is only after increasing the beam current above the threshold in a ratio of approximately 3 to 2 that for a 1.6 μ sec pulse, the plane of polarization of the break-up becomes random. This observation can be understood from the fact that the Q is higher in the direction perpendicular to the input coupler where no leakage occurs and that the resonant build-up is greater

in that direction. While definitive Q and shunt impedance measurements still remain to be made, it appears that the value of Q_0 is between 7000 and 10,000 in the vertical plane and that Q_L , the loaded Q in the horizontal plane, is roughly two-thirds of this value. These somewhat unsatisfactory results were obtained from a variety of Q measurements, one of which is illustrated in Fig. 17. This value was obtained by matching the input to the accelerator section at 4139.6 MHz with a slide screw tuner and by measuring the ringing time response to a very short input pulse. It should be noticed from Fig. 17 that the one-way travel time of the resonant wave is of the order of 50 nanosec. Hence, for the resonant effect to become predominant, it is necessary that the beam pulse be at least twice as long. This result was actually observed on the accelerator: for very short injector pulses, the beam still breaks up in one plane but the orientation of the plane is random from pulse to pulse.

Microwave Beam Tests

As discussed in the Introduction, a large number of experiments were performed with the beam itself. Although they are not entirely independent, these experiments have been divided into two categories: microwave experiments and focusing experiments. This section of the report deals with the microwave experiments, the next one with the focusing experiments.

Referring again to Fig. 4, it is seen that a number of microwave devices were installed along the machine. After it was understood how the various frequencies associated with break-up were interrelated, it became evident that microwave cavities capable of interacting with a transverse modulation on the beam could be built either at L-band or at C-band. As seen from the figure, there are presently two vertical cavities at the 40-foot point (one at L and one at C-band), two vertical L-band cavities at the end of sector 3, and two vertical and two horizontal C-band cavities at the end of sector 5. For an extended period, while the Beam Switchyard was being completed, the beam was stopped at the end of sector 19 and a variety of devices were installed beyond that point in air. These are also shown in Fig. 4: one vertical and one horizontal C-band cavity, various types of loops, and a short accelerator section. More accurate data on the growth of the phenomenon could have been obtained if it had been possible to install such cavities at the end of every sector along the machine. However, as already mentioned, the cost of building and installing a large number of these devices would have been prohibitive. The existing equipment, however, was sufficient to carry out a large number of diagnostic experiments, such as the measurement of the frequencies present on the beam and the wave shapes of the induced power, and to perform various feedback experiments. All of these and others will be described below.

The cavities are sketched in Figs. 18 and 19. The 4140 MHz cavities were built strongly over-coupled ($Q_L \sim 1.5$) but for a few experiments were made resonant with double-stub tuners ($Q_L \sim 200$). The L-band cavities were tunable over a narrow range by means of an extra set of probes not shown in the figure. By changing the loads on these probes, it was possible to vary their loaded Q from 4000 down to approximately 200.

Figure 20 shows four photographs of rf pulses induced by the beam at 1284 MHz in the L-band cavities at the end of sector 3. As the beam current is increased, it is seen that the rf signal not only increases but also becomes somewhat more stable.

Several attempts were made to try to eliminate or at least to reduce the beam break-up effect through feedback. The term "feedback" actually gives a poor description of the experiment because in no case would it be reasonable to pick up the signal induced by the beam at a given point and to feed it back into an upstream cavity. This is true because it would require a negative time delay to feed back the coherent signal in time to have any effect. This difficulty with time delays is also inherent in any "feed-forward" experiment such as the one that was performed and is illustrated in Fig. 21. As will be seen, a large amount of gain is required to show any effect at all and the time delay contributed by the amplifiers, filters, cables, etc., is of the order of 50 nanosec minimum. Because of the complexity of the set-up, it was at first necessary to install the equipment in the klystron gallery to be able to have manual access to the various adjustments. This increased the necessary length of the cables to the cavities and lengthened the time delays to close to 100 nanosec. Furthermore, it is difficult to find high-gain high power amplifiers at 4140 MHz. The feedback experiment was attempted at that frequency with two TWT amplifiers but failed because of insufficient gain. Since no high-power amplifier could be found at this frequency, it was decided to repeat the experiment at 1284 MHz. The layout shown in Fig. 21 was used at 1284 MHz. After a fair amount of experience was gained with this equipment, particularly the 10 kW pulsed output stage, the entire set-up was lowered into the accelerator housing and installed next to the in-line cavities. Only the controls and triggers remained upstairs. Under these conditions, the feedback experiment achieved some measure of success. Some of the results are illustrated in Fig. 22. The left-hand photograph shows the effect of pulse shortening at the end of sector 6; the right-hand photograph shows the elimination of pulse shortening at the same point by feedback at the end of sector 3. This improvement was obtained with approximately 100 db of gain in the amplifier chain and proper adjustment of the phase shifter. Presumably, the level of the feedback signal was such that the transverse momentum in sector 3 was either cancelled or slightly inverted. In the first case, the cancellation would not have removed the amplitude modulation; in the second case, it would have removed some of the amplitude modulation by imparting new momentum modulation in the opposite direction. Unfortunately, the pulse shortening could not be eliminated beyond sector 7 with this set-up. When the current was increased beyond 43 mA, pulse-shortening even reappeared at sector 6. Hence, the feedback worked only over a very short distance and a narrow range of currents. While these results are not entirely discouraging, several conclusions can be drawn:

(a) To make the feedback system workable, several stages would be necessary along the machine, perhaps as many as 5 or 10.

(b) Since it appears from other experiments that at slightly higher currents, the break-up can take place in any polarization, it would be necessary to install equivalent set-ups with horizontal cavities. This would double the number of required stages.

(c) The whole feedback chain may have to be of a wider bandwidth than obtainable, because of the phase shifts and higher frequencies liable to appear.

(d) There may be additional difficulties from the fact that the time variation of the signal induced in the cavities changes with the current level. Hence, it may be necessary to re-adjust the gain and perhaps even the pulse shape of the last amplifier to achieve the proper compensation.

(e) In view of all these facts, the feedback system would probably cost a minimum of \$300,000, and its operational complexity may be prohibitive. Even if workable, its cost does not compare favorably with the cost of other proposed remedies and hence the scheme cannot be adopted light-heartedly. While further research on the feedback scheme will continue at SLAC for some time, it is now being given low priority.

Another idea proposed by many linear accelerator specialists is to build into the accelerator sections passive devices capable of attenuating or suppressing the TM_{11} mode. It has been conjectured that while the choice of the constant-gradient design was a good one, the choice of the $2\pi/3$ mode perhaps was not, because the beam interaction would not have been as close to the edge of the TM_{11} passband if the earlier $\pi/2$ mode had been retained. It has been suggested that the break-up threshold might be increased on the two-mile accelerator if two or three sectors at the beginning of the machine could be rebuilt using $\pi/2$ rather than $2\pi/3$ sections. In this case, whatever transverse modulation would be impressed on the beam at the beginning of the machine, the frequency would be different from 4140 MHz. The 4140 MHz modulation would then start at a much higher beam energy and the gain would be reduced. While in theory this solution might be workable, it would require rebuilding the whole front end of the accelerator and, in addition to the cost involved, it would entail a considerable period of accelerator down-time. Consequently, it cannot be contemplated at this time. Another possibility would be to modify the existing accelerator sections by means of some external coupling mechanism which would, in effect, decrease the shunt impedance of the TM_{11} mode at the beginning of the accelerator. Many ideas along this line have been suggested and one of them is illustrated in Fig. 23. This short constant-gradient input subassembly was installed in air at the end of sector 19 and several beam tests were performed with it. The effect of the two couplers at 4140 MHz was observed under various conditions of matching and shorting. The key experiment was to compare the 4140 MHz signal level inside this subassembly under two conditions: (i) with the output of the 4140 MHz upstream coupler matched and (ii) with the output of the same coupler shorted at such a position that an effective short appeared across the side aperture of cavity No. 1 in the disk-loaded waveguide structure. Such an operation is rather complicated because of the interaction between the 4140 MHz couplers and the adjacent 2856 MHz couplers. The best result obtained was a reduction in field strength at 4140 MHz inside the accelerator section by a factor of 3 when the 4140 MHz coupler was matched. Again, while this scheme might be workable, it is rather complicated. It requires intervention into the vacuum system and may create new problems due to the coupler asymmetry inherent in the design. Furthermore, it may cure beam break-up only in the vertical direction, and the effect may then reappear a few milliamperes higher in the horizontal direction. For all these reasons, this

solution is also being given low priority.

Another attempt to increase the charge transmitted through the accelerator is illustrated in Fig. 24. The basic idea was to take advantage of the build-up and decay time of the TM_{11} mode and to see if by pulsing the injector intermittently during the $1.6 \mu\text{sec}$ available for the beam, it was possible to transmit more total charge. The example in the figure shows two short injector pulses. In another experiment as many as three pulses were attempted, but in no case did the total charge transmitted surpass that obtained with a lower amplitude injector pulse present throughout the $1.6 \mu\text{sec}$ as shown. In fact, not only did the short pulses have an effect on each other because the TM_{11} mode had not sufficiently decayed in the inter-pulse period, but there appeared to be a sharp decrease in transmitted current for very short pulses (less than 100 nanosec). This result further confirms that the charge conservation law begins to break down for very short pulses. It is not entirely clear to what extent this result is caused by beam break-up or by beam loading. In any case, it was very difficult to transmit beam pulses of more than 80 mA through the entire machine for any pulse length.

Beam Focusing Experiments

When the beam break-up effect at SLAC was first discovered, the mechanism was not immediately understood and consequently its interaction with focusing along the machine was not clear. A few preliminary tests appeared to show that the effect was not a function of focusing strength, and this fact was erroneously reported in Ref. 1. From evidence available from beam break-up effects observed in earlier one- or two-section machines, it was thought that if the effect could somehow be quenched in the first one or two accelerator sections, this would be sufficient to increase the transmitted current by at least an order of magnitude. However, these assumptions soon proved to be wrong and were abandoned in favor of the theoretical model now adopted, based on a multi-section cumulative interaction. As can be guessed, all experiments attempting to strongly focus the beam in the injector or to collimate it after the first 10-foot section failed to give any improvement. Similarly, it was also shown that increasing the gun injection voltage from 50 to 80 kV had no effect on the break-up threshold.

Subsequently, more careful tests have been made with the quadrupole triplet system available at the end of each accelerator sector. The layout of a typical drift section is shown in Fig. 25. There are three quadrupoles on this drift section, two of the A type and one of the B type, which is twice as strong. The maximum presently available current for these quadrupoles is 7 Amps. Because of their construction, the A-quadrupoles saturate at about 12 Amps whereas the B-quadrupoles saturate at about 15 Amps. Quadrupole triplets had originally been selected because, in case of alignment instabilities, they produce less steering than doublets of the same length. It was found, however, that the alignment of the drift sections in the machine is very good and that it does not change as a function of time. Consequently, roughly two months after machine turn-on, an experiment was performed where the quadrupoles were rewired as doublets, leaving out the middle B-quadrupole entirely. The doublet focusing system worked just as well, and with twice the spacing but half the magnet strength, the

focusing strength of the doublets remained the same as that of the triplets. The data given in the next figures summarize the effect of focusing on the beam break-up threshold. Figure 26 gives two examples, one for a 3.7 GeV beam accelerated in the first fifth of the machine and then drifting, and one for a 16.8 GeV beam, uniformly accelerated along the total length. Each point on the two straight lines gives the maximum quadrupole current to which the power supplies were set along the machine. The 12 Amp point was obtained by temporarily using extra power supplies. In all cases, linearly increasing focusing was used from the injector up to the noted value and the betatron phase shift shown for the corresponding abscissa was an average obtained over the full length of the machine. It is known that if the focusing strength increases far beyond $\pi/2$ betatron phase shift per sector, the beam is thrown into the accelerator walls before it can be re-focused by the next quadrupole doublet. The linear relationship shown in Fig. 26 indicates one of the most obvious remedies that can be adopted to increase the transmitted current through the machine, i.e., stronger focusing. Hence, if enough focusing were available to operate the quadrupole doublets everywhere at a strength corresponding to a betatron phase shift per sector of $\pi/2$, it should be possible to increase the transmitted current to about 35 mA peak. Figure 27 shows that it is actually possible to exceed the $\pi/2$ phase shift somewhat and still increase the transmitted current. Another fact, also illustrated by Fig. 27, is that as long as the focusing does not exceed the $\pi/2$ point too much, it is possible to change the spacing between quadrupoles and obtain approximately the same transmitted current provided the betatron wavelength is preserved.

Evaluation of these results, both on theoretical and experimental grounds, has led to the corrective program which is presently being adopted as the simplest and most inexpensive cure for beam break-up. Since the B-quadrupoles shown in Fig. 25 are no longer used for triplets, approximately 44 of these magnets are now available on the machine (including 24 magnets from the special positron focusing system). These magnets will be removed from the accelerator, and drift sections with B-doublets will gradually be rebuilt and re-installed in the machine from sector 10 to 30. With new power supplies having a capability up to 15 Amps, the future focusing system from sector 10 on, as shown in Fig. 28, will be from 3 to 4 times stronger than the present doublet system which uses only A-magnets. This increased focusing capability will permit linearly increasing the focusing strength as shown in Fig. 26, up to an equivalent current of 25 Amps, and should yield a transmitted beam current at least 50% higher than presently obtained. In addition, the removal of A-magnets from the end of the machine will make available about 40 of these for other uses. Since strengthening the focusing in the early part of the machine is probably most effective in increasing the beam break-up threshold, it is being planned to slightly modify these available A-magnets and to install them as singlets in sectors 1 to 6, every 40 feet, as shown in Fig. 28. The combination of these two steps should easily permit increasing the present transmitted current by more than 100%, thereby meeting the original specification of 50 mA of peak current. It should also allow one to increase the focusing for low energy beams without running into stop-bands.

The advantages of this entire program are that it can be achieved gradually, that its results can be

measured as it is being carried out, that it requires no new magnet procurement, and finally, that it can be implemented without any appreciable down-time on the accelerator. In summary, this two-step program has been adopted as the official cure for beam break-up. While it does not constitute the most elegant solution, it has the further advantage that it is certain to work and to take care of both known and unknown transverse modulations that may appear when the accelerator current is gradually increased.

In addition to this program, attempts are still being made to look at other solutions making use of focusing, and in particular, to understand the effects of sextupoles or octupoles. The role of these higher-order focusing magnets can be understood by noticing that electrons in a bunch going through such magnets at different distances from the accelerator axis will be caused to cross over the axis at different downstream distances from the magnet. Simple calculations show, for example, that a sextupole with 275 gauss-cm at one cm will cause a 1-GeV electron at 1/2 cm from the axis to cross over after 250 meters of travel, whereas a similar electron at 1/4 cm from the axis would cross the axis at twice that distance. Hence, it would appear that if such sextupoles were installed along the machine at frequent enough intervals, their presence would flip the phase of the transverse modulation of the beam at different points along the axis for different radial amplitudes and the resulting mixing effect would decrease the rate of the TM₁₁ build-up. A rather simple experiment of this kind was performed on the machine, using three small fan-motor stators purchased for about \$12 each and installed in sectors 6, 7, and 8. One of them is shown in Fig. 29. For reasons that are not entirely understood at this point, experiments with these sextupole magnets did not show any effect. A special computer program is presently being developed to calculate the strength of the sextupole focusing that would be required before the effect would become noticeable.

Other ideas have been proposed along this line such as time-varying quadrupoles using ferrite cores which could be resonated several times within the available 1.6 μ sec or microwave dipoles which would use a phase-modulated signal to obtain the desired mixing effects. According to theoretical calculations,² the former does not appear to be promising, and the latter showed no effect when it was tried at the beginning of the machine.

Conclusion

The presently adopted program to correct beam break-up by increasing the quadrupole focusing strength and periodicity along the machine seems to provide the simplest solution for the two-mile accelerator. On the other hand, if one were to build a new accelerator of this type today, perhaps more elegant solutions might be adopted, either by modifying the accelerator structure to displace the TM₁₁ mode to a higher frequency, or by quenching it altogether with slots or additional irises in the structure. In the future, new long linear accelerators or super-conducting accelerators of medium length but very long pulse length will no doubt make use of solutions of this kind. In the meantime, it should be possible to use the two-mile SLAC accelerator to gain further knowledge about the basic noise or shock excitation which starts the effect, and to provide experimental verification for the theoretical beam break-up investigations which are presently

underway. Aside from the high energy physics program which is now starting at SLAC, many interesting hours will no doubt yet be spent on the accelerator such as the one illustrated in the photographs of the last figure, taken when the beam was first turned on in April, 1966.

References

1. W.K.H. Panofsky, R. B. Neal, and the staff of the Stanford Linear Accelerator Center, "Electrons Accelerated to the 10- to 20-GeV Range," *Science*, Vol. 152 (June 1966).
2. R. H. Helm, "Computer Study of Wave Propagation, Beam Loading and Beam Blowup in the SLAC Accelerator," paper presented at the 1966 Linear Accelerator Conference at Los Alamos.
3. R. Borghi, A. Eldredge, G. Loew, R. Neal, "Design and Fabrication of the Accelerating Structure for the Stanford Two-Mile Accelerator," *Advances in Microwaves*, Academic Press, New York.

TABLE I

Dimensions of Constant Gradient 10-Foot Accelerator Section

All dimensions in inches: 2a = disk hole diameter (upstream end of cavity)
2b = inside cylinder diameter

Cavity No.	2 a	2 b	Cavity No.	2 a	2 b
1	1.0323	3.2844	43	.9217	3.2548
2	1.0300	3.2838	44	.9185	3.2540
3	1.0277	3.2831	45	.9153	3.2532
4	1.0254	3.2824	46	.9121	3.2524
5	1.0231	3.2817	47	.9089	3.2517
6	1.0207	3.2810	48	.9056	3.2509
7	1.0183	3.2803	49	.9023	3.2501
8	1.0159	3.2797	50	.8990	3.2493
9	1.0135	3.2790	51	.8956	3.2485
10	1.0111	3.2783	52	.8922	3.2477
11	1.0087	3.2776	53	.8888	3.2469
12	1.0063	3.2769	54	.8854	3.2461
13	1.0039	3.2762	55	.8819	3.2453
14	1.0015	3.2756	56	.8784	3.2444
15	.9991	3.2749	57	.8749	3.2436
16	.9967	3.2742	58	.8713	3.2428
17	.9943	3.2735	59	.8677	3.2419
18	.9918	3.2728	60	.8640	3.2411
19	.9893	3.2721	61	.8603	3.2403
20	.9868	3.2714	62	.8565	3.2394
21	.9843	3.2707	63	.8527	3.2385
22	.9817	3.2701	64	.8488	3.2377
23	.9791	3.2694	65	.8449	3.2368
24	.9765	3.2687	66	.8409	3.2359
25	.9739	3.2680	67	.8369	3.2350
26	.9712	3.2673	68	.8329	3.2341
27	.9685	3.2666	69	.8288	3.2332
28	.9658	3.2659	70	.8246	3.2323
29	.9631	3.2652	71	.8204	3.2314
30	.9603	3.2645	72	.8161	3.2305
31	.9575	3.2638	73	.8117	3.2296
32	.9547	3.2631	74	.8072	3.2287
33	.9518	3.2623	75	.8027	3.2277
34	.9489	3.2616	76	.7981	3.2268
35	.9460	3.2609	77	.7934	3.2258
36	.9431	3.2602	78	.7886	3.2248
37	.9401	3.2594	79	.7836	3.2238
38	.9371	3.2587	80	.7786	3.2228
39	.9341	3.2579	81	.7735	3.2218
40	.9310	3.2572	82	.7682	3.2208
41	.9279	3.2564	83	.7628	3.2198
42	.9248	3.2556	84	.7573	3.2187
			85	.7517	---

Outside diameter: 3.998
 Disk thickness: 0.230
 Disk spacing: 1.378
 Iris rounding: Radius: 0.1215; Flat land inside iris: 0.0310

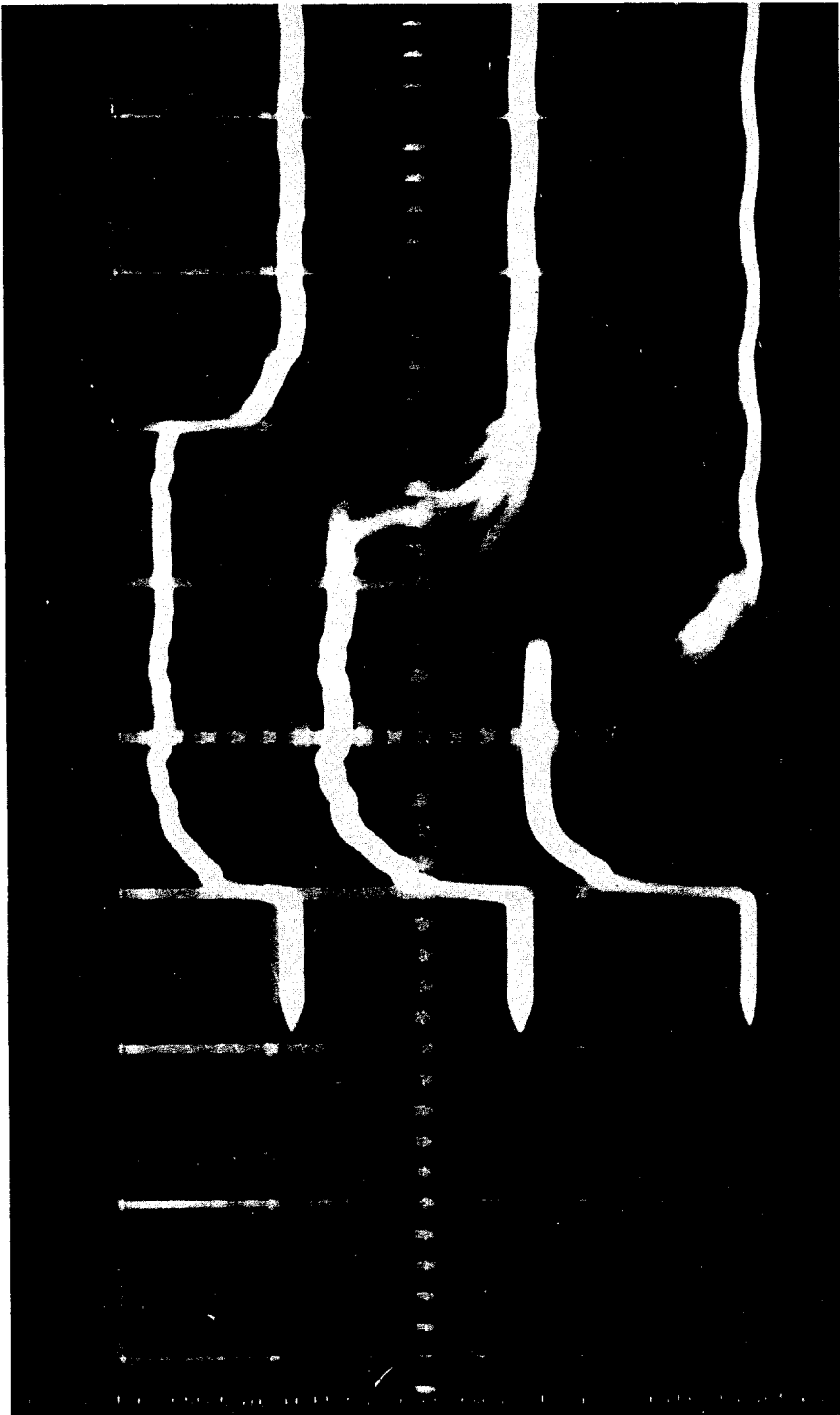
Couplers

Endplate: Thickness 0.7629; Hole diameter 0.7517

Radius (b)	Input Coupler	1.5458	Output Coupler	1.5655
Waveguide iris aperture	Input Coupler	1.130	Output Coupler	0.900
Offset	Input Coupler	0.155	Output Coupler	0.0800

LIST OF FIGURES

1. Beam pulses below and above **break-up** threshold.
2. Linear Q profiles below and above **break-up** threshold (energy: 5 GeV, pulse length: 1.6 μ sec).
3. PLIC profile for beam break-up at sector 12 (5 GeV, 1.6 μ sec).
4. Layout of entire accelerator with beam break-up experiments.
5. Mechanism leading to beam break-up.
6. Beam pulses in sector 20 (~ 1 GeV).
7. Beam break-up current vs. inverse length (energy = 0.6 MeV).
8. Beam break-up current vs. inverse length (all sectors at 225 MeV/sector).
9. Beam break-up current vs. energy.
10. Time to beam break-up vs. $(tiz)^{1/3}$ (six sectors per betatron wavelength).
11. Transverse displacement modulation due to beam break-up as a function of the quantity $(iz)^{1/3}$.
12. Typical SLAC microwave technician showing length of troublesome cavities in typical constant-gradient accelerator section.
13. $\omega - \beta$ diagrams for the TM_{11} mode measured at three different locations in the ten-foot constant-gradient section.
14. Electric field intensity in ten-foot section at 4139.6 MHz (cold test, horizontal excitation through coupler).
15. VSWR looking into input of ten-foot accelerator section.
16. Passband of ten-foot constant-gradient section for TM_{11} mode.
17. Measurement of Q at 4139.6 MHz by ringing technique (matched case, $Q_L = Q_o/2$).
18. 4140 MHz cavities used in beam break-up experiments (both cavities are 7.9" long).
19. 1284 MHz cavities used in beam break-up experiments.
20. Rf pulses induced at 1284 MHz in sector 3 cavities (energy ~ 1 GeV).
21. Beam break-up feedback experiment.
22. Effect of feedback at 1284 MHz.
23. Constant-gradient input subassembly with both 2856 and 4140 MHz couplers.
24. Example of two interlaced beams, one of which consists of two short (~ 150 nsec) sub-pulses.
25. Layout of a typical drift section.
26. Beam break-up current vs. focusing.
27. Beam break-up current vs. betatron phase shift per sector.
28. Present and future quadrupole deployment.
29. \$12.00 sextupole magnet.
30. Emotions around the first SLAC beam (April 21, 1966).



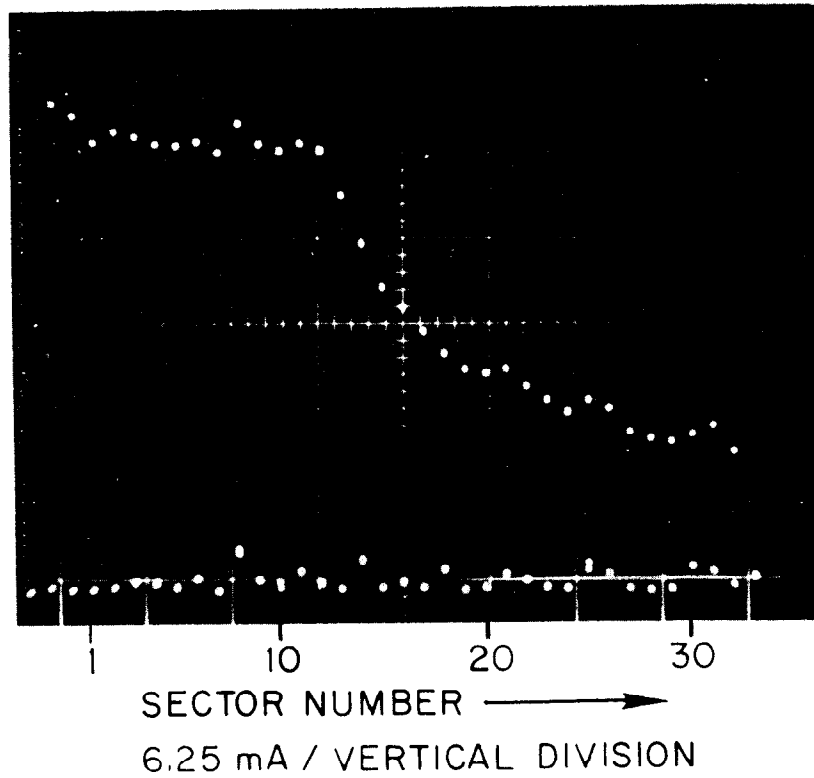
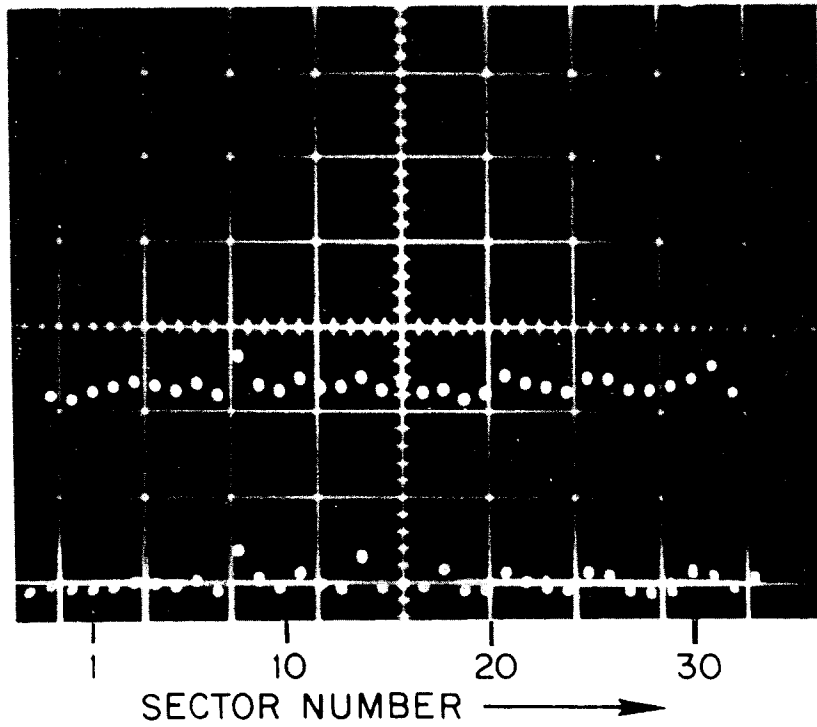
0.5 μ sec / DIVISION \longrightarrow

FIG. 1--BEAM PULSES BELOW AND ABOVE
BREAK-UP THRESHOLD

6006A

X

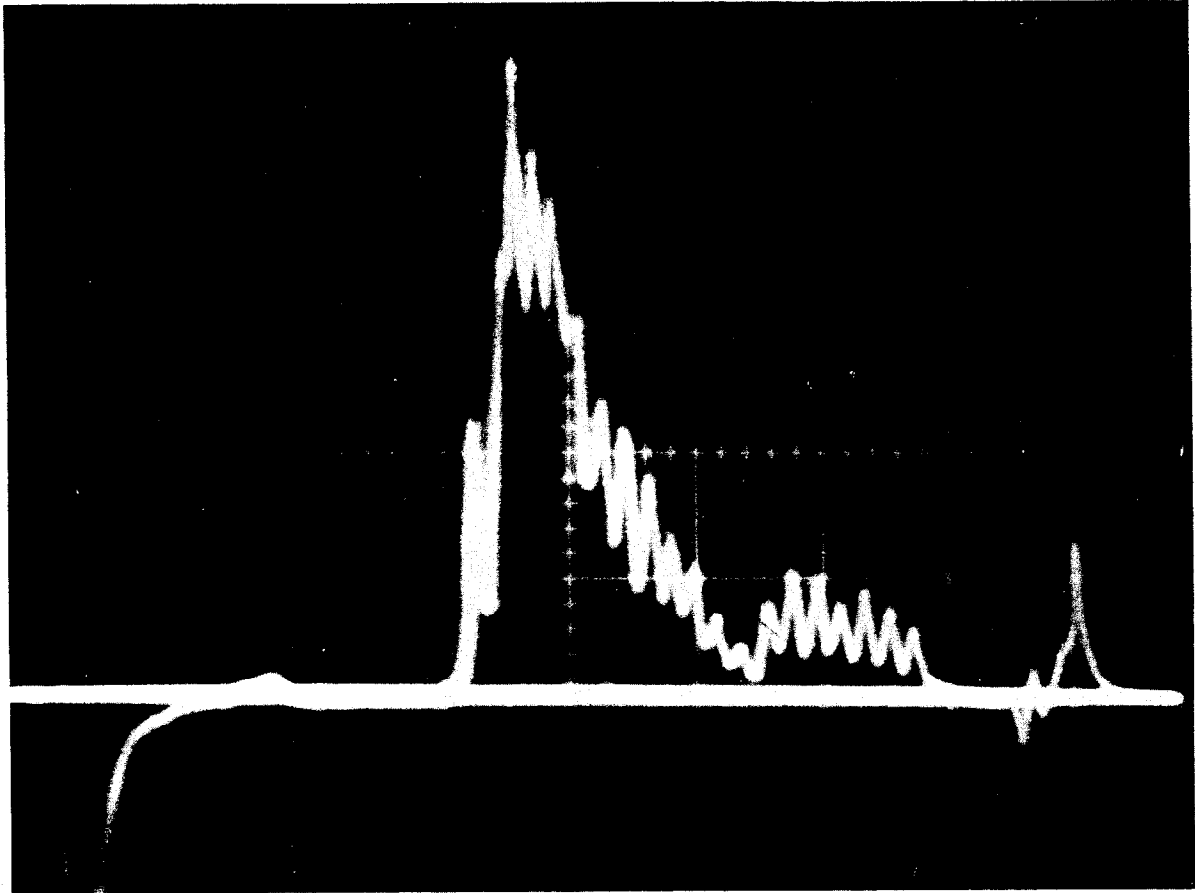
167 M35-16



167 M 35-10

600-5-A

FIG. 2--LINEAR Q PROFILES BELOW AND ABOVE BREAK-UP THRESHOLD (ENERGY : 5 GeV, PULSE LENGTH 1.6 μ sec)



0 10 20 30
SECTOR NUMBER

PLIC PROFILE FOR BEAM BREAK-UP AT
SECTOR 12 (5 GeV, 1.6 μ sec PULSE)

FIG. 3

600-3-A

167 m35-15

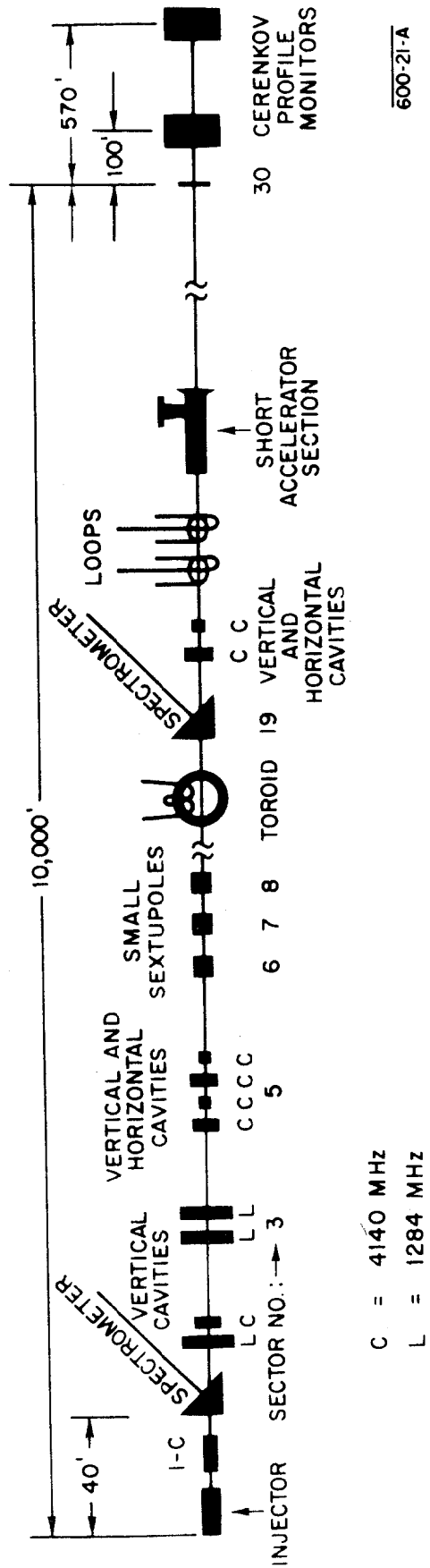


FIG. 4 -- LAYOUT OF ENTIRE ACCELERATOR WITH BBU EXPERIMENTS .

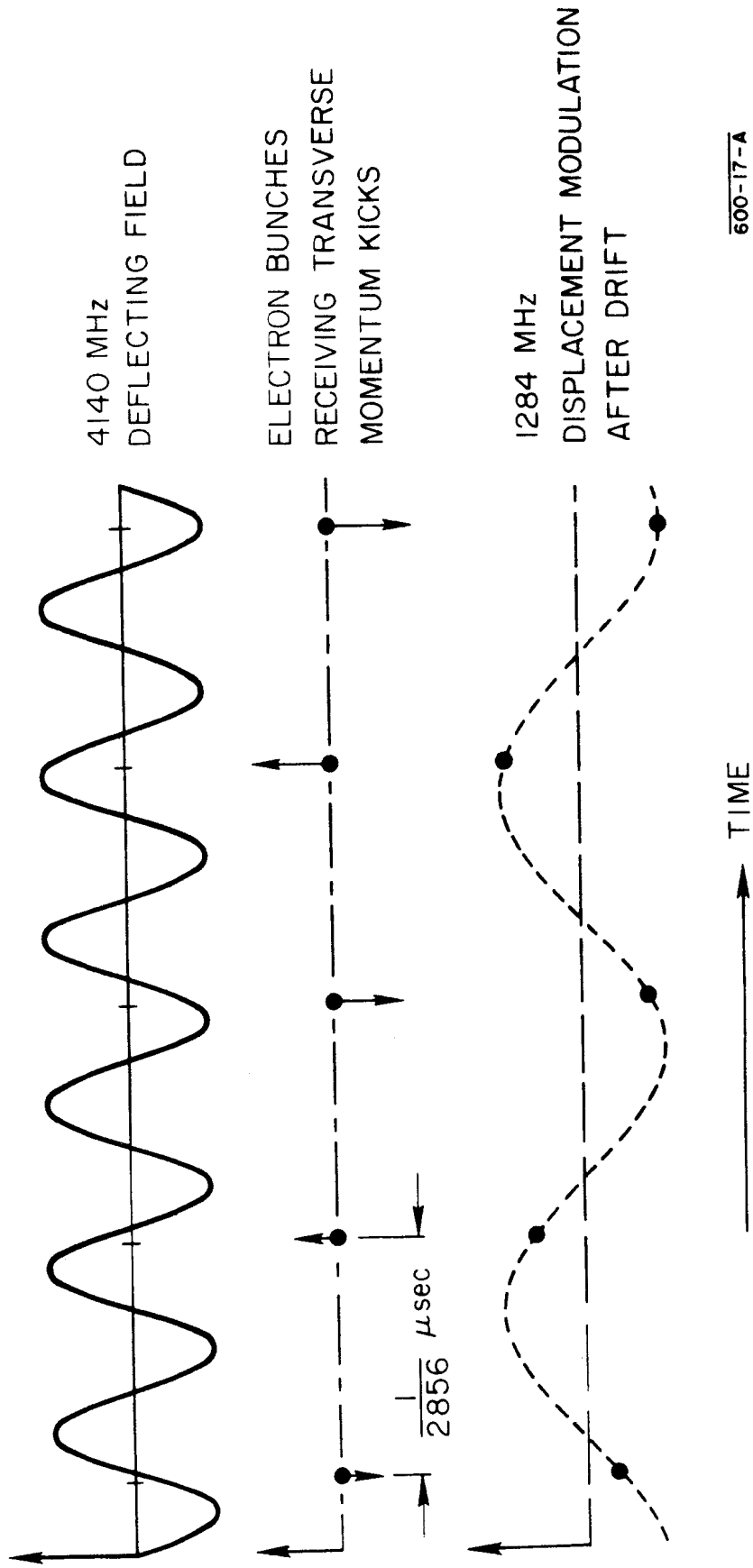
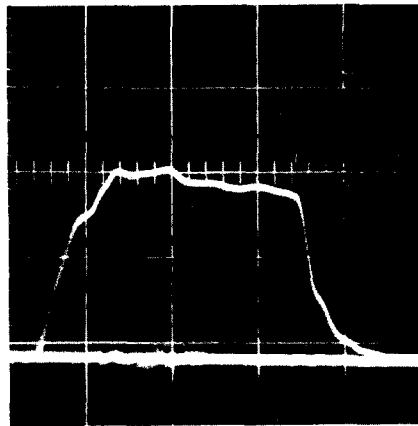
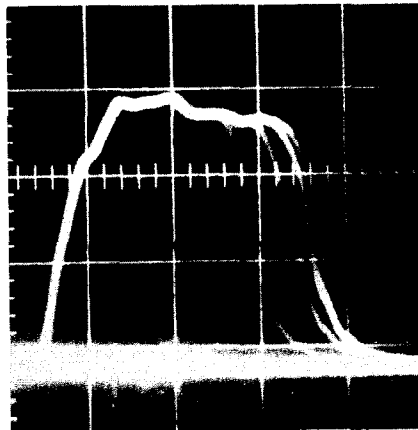


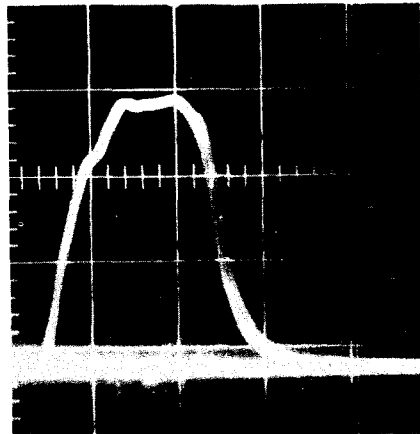
FIG. 5 -- MECHANISM LEADING TO BEAM BREAK-UP



6.5 mA
BELOW BBU



10.1 mA
NATURAL BBU

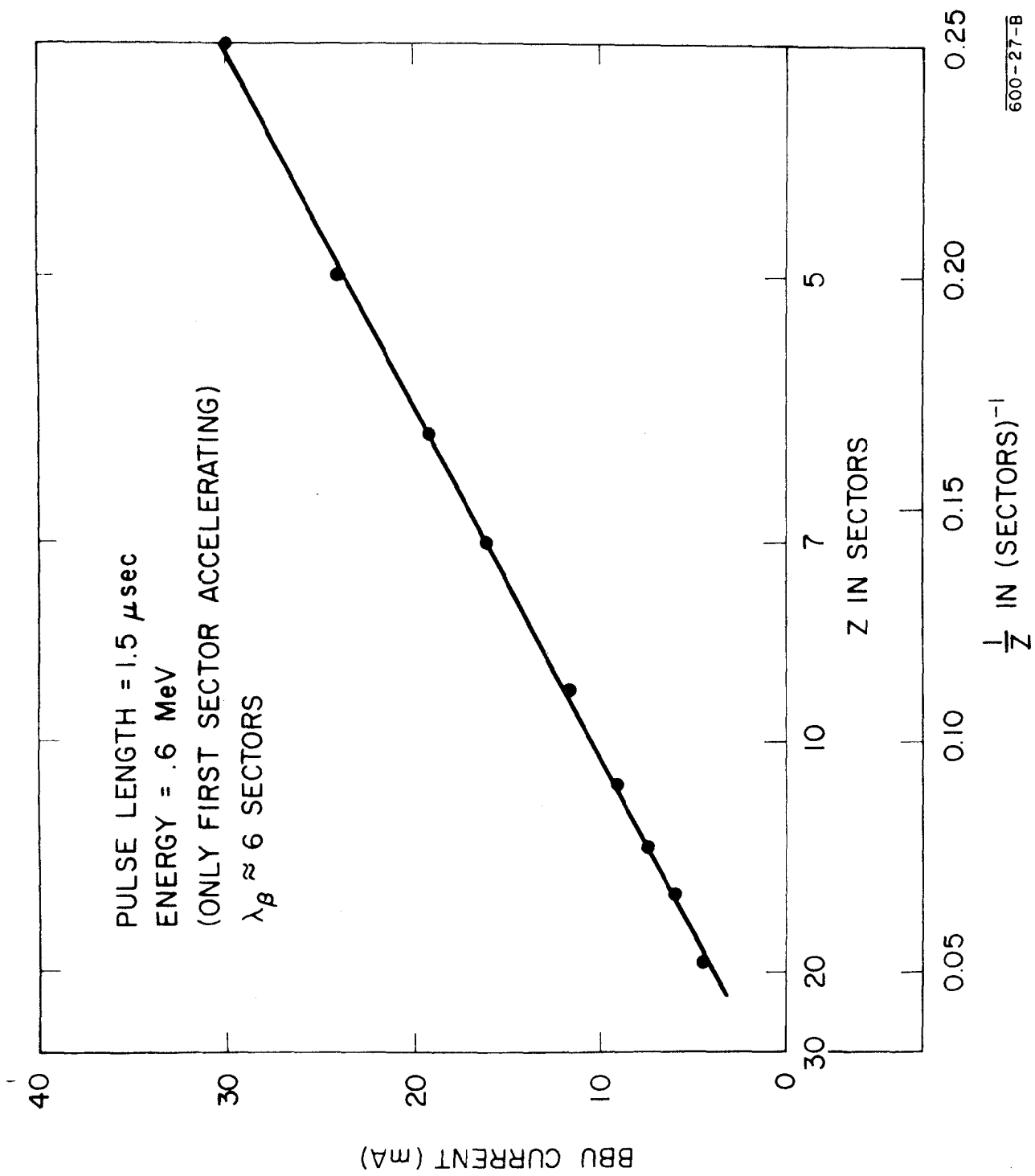


10.1 mA
BBU STIMULATED
AT 4140 MHz
AT 40' POINT

0.5 μ sec / div.

600-11-A

FIG. 6--BEAM PULSES IN SECTOR 20
(~ 1 GeV)



600-27-B

FIG. 7 -- BEAM BREAK-UP CURRENT vs INVERSE LENGTH

X

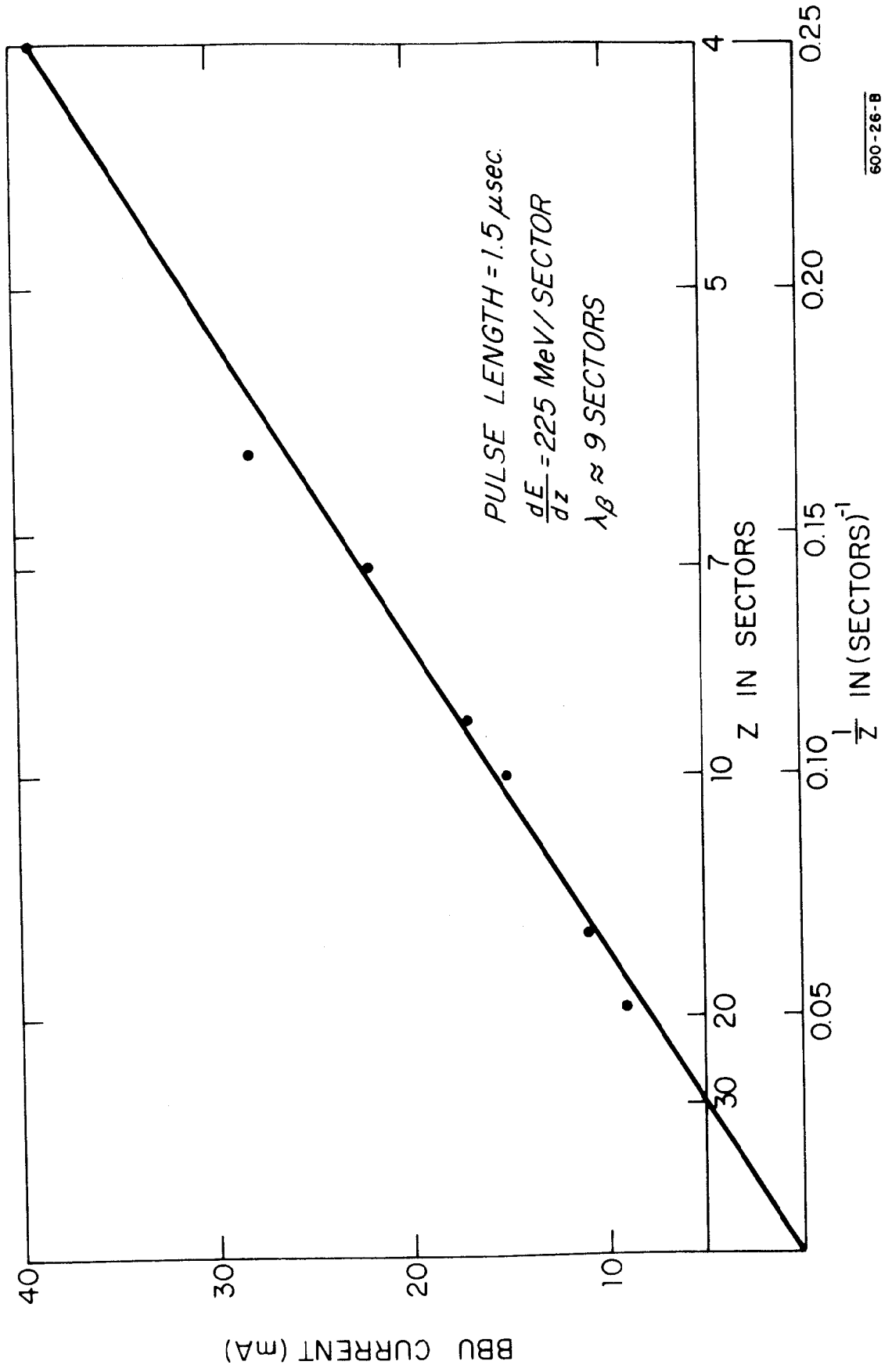


FIG. 8-- BEAM BREAK-UP CURRENT vs INVERSE LENGTH

167 m35 - 25

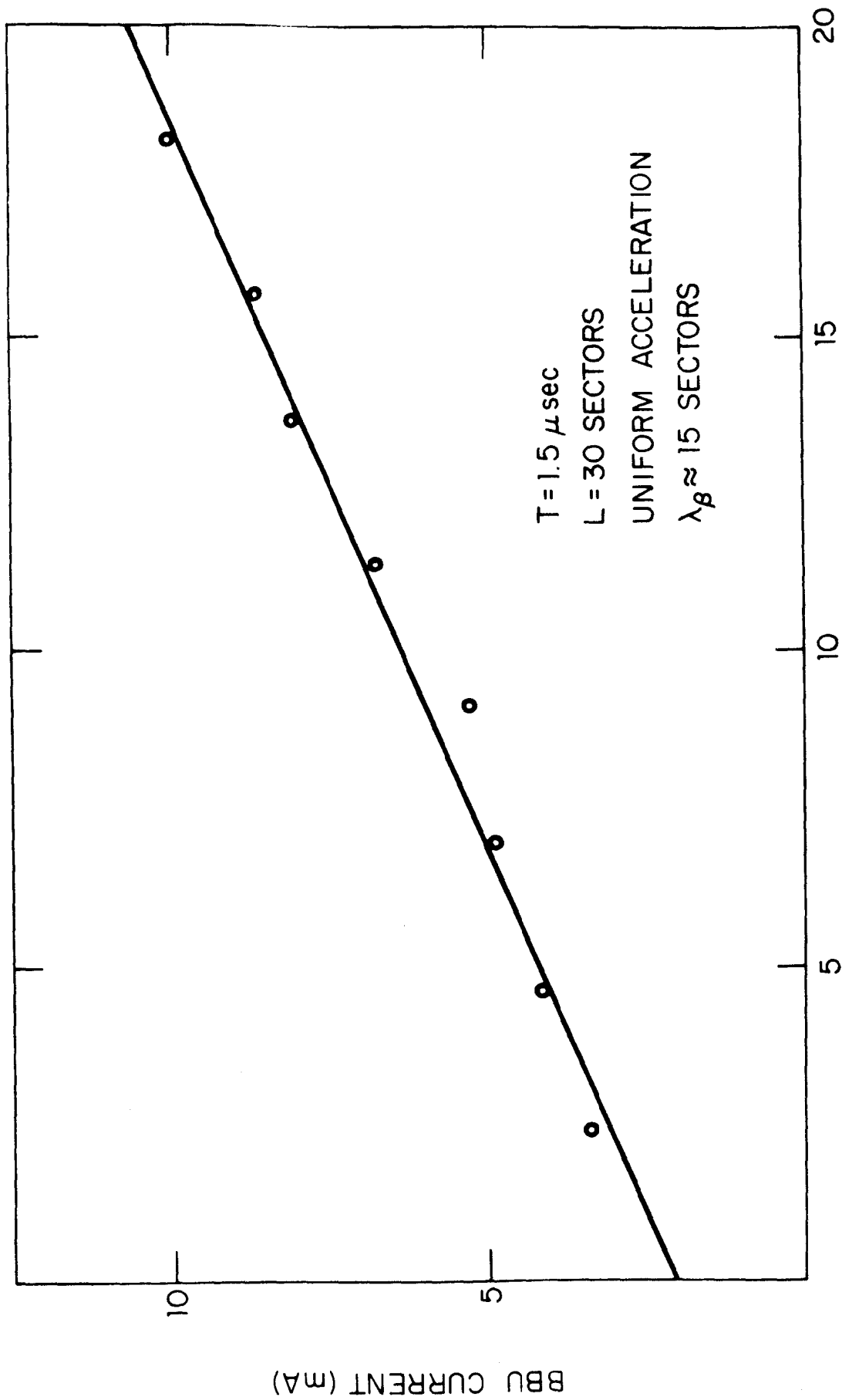


FIG. 9 -- BBU CURRENT vs ENERGY

600-14-B

167 M35-8

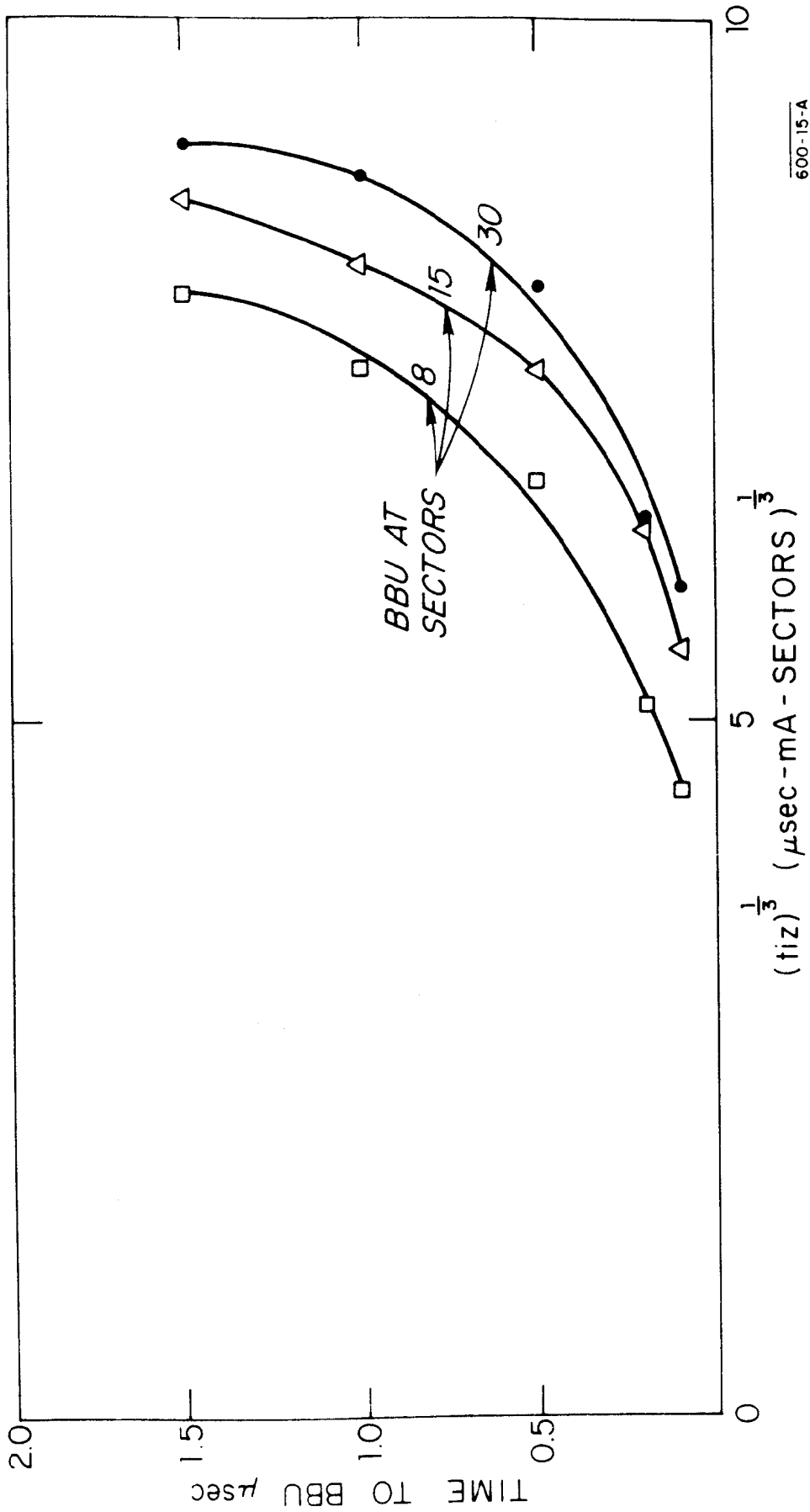


FIG. 10 -- TIME TO BBU vs $(tiz)^{\frac{1}{3}}$

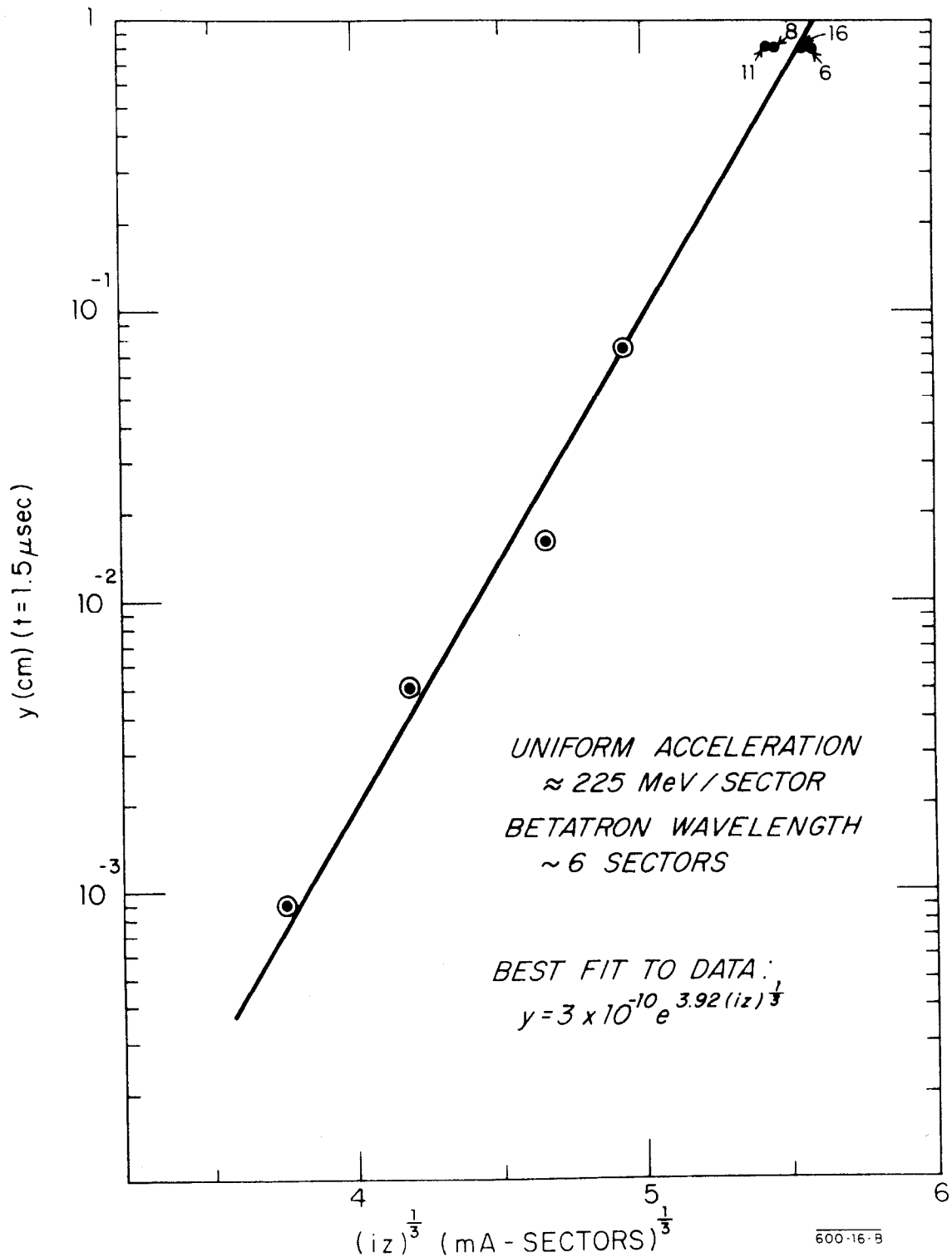


FIG. 11 -- TRANSVERSE MODULATION IN BBU AS A FUNCTION OF $(iz)^{1/3}$. CIRCLED POINTS MEASURED BY OBSERVING INDUCED POWER IN C-BAND PROBE AT END OF SECTOR 5. NUMBERED POINTS ARE THE ONSET OF SCRAPING AT SECTOR INDICATED.

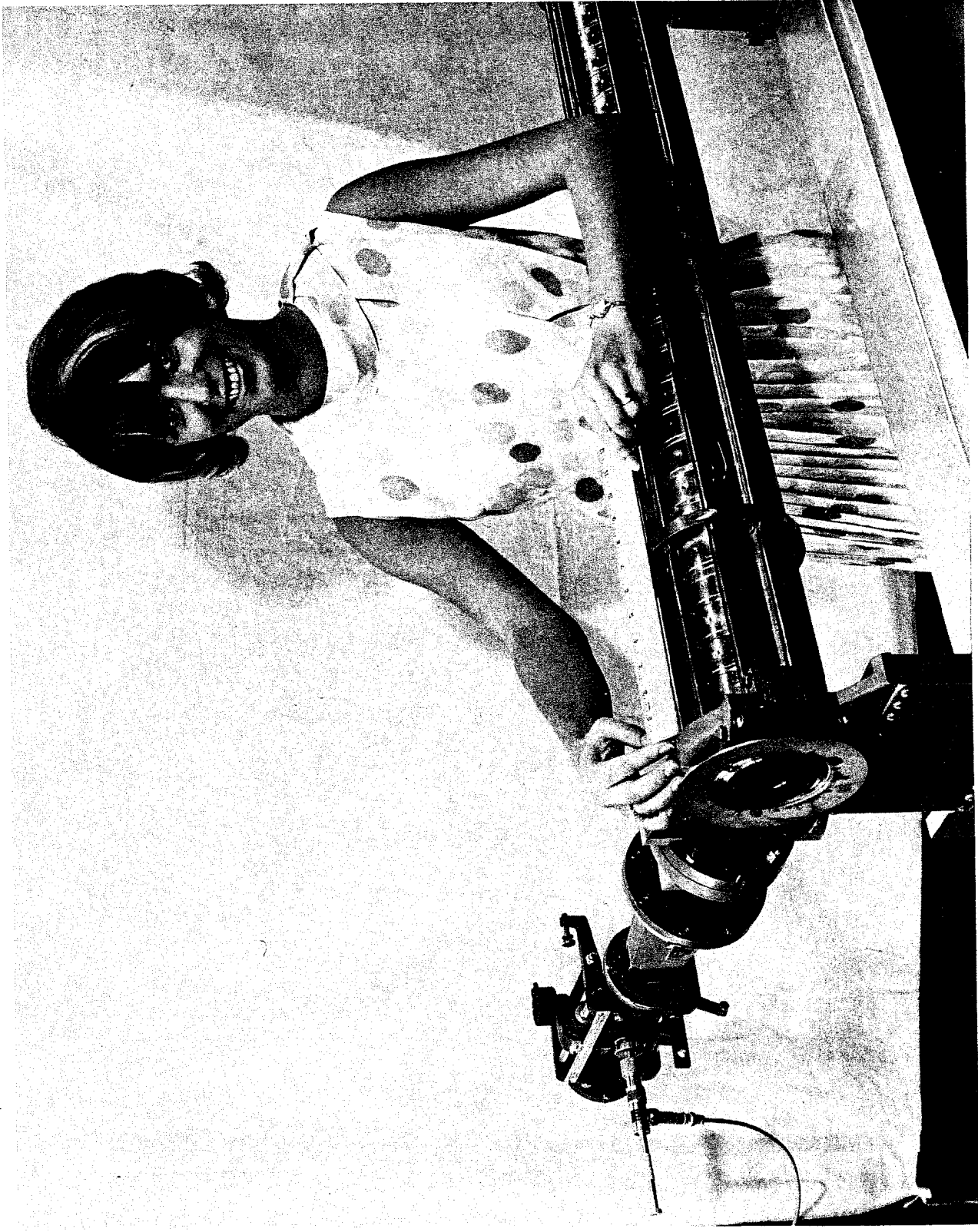
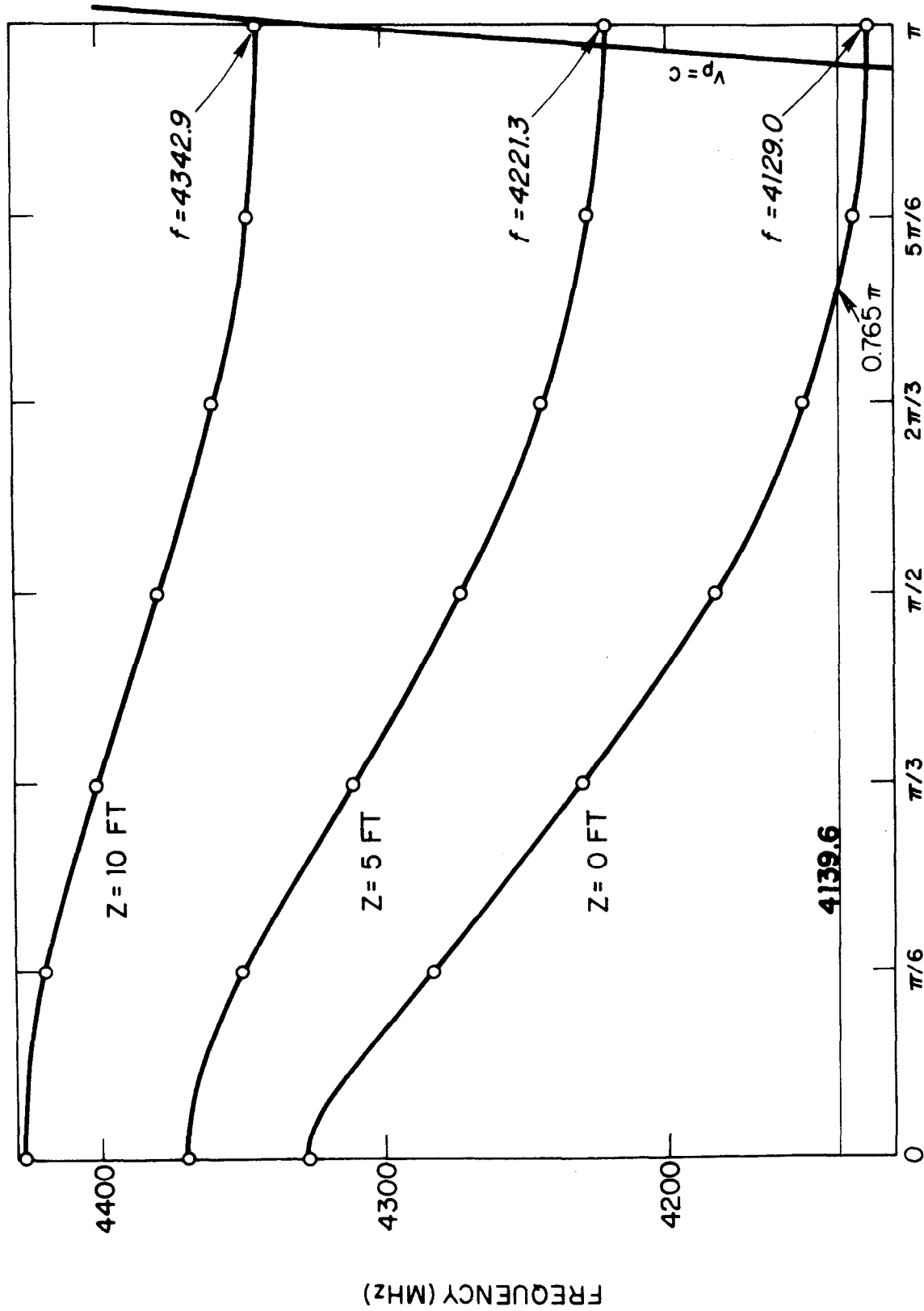


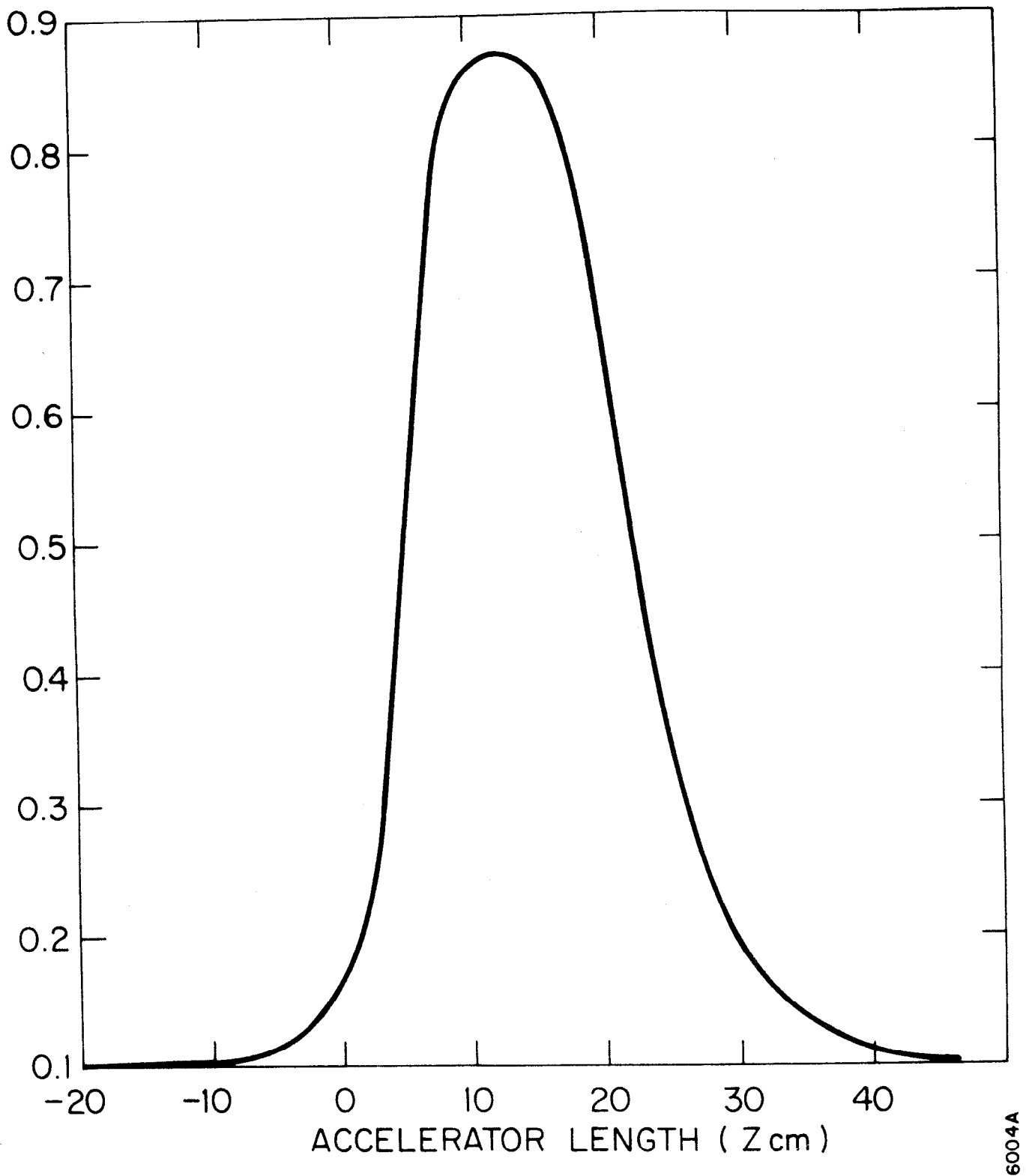
Fig. 12--Typical SLAC microwave technician showing length of troublesome cavities in typical constant-gradient accelerator section.



600-1-B

PHASE SHIFT PER CAVITY

FIG. 13 -- BRILLOUIN DIAGRAMS FOR TM_{11} - MODE AT THREE LOCATIONS IN CONSTANT - GRADIENT SECTION



ELECTRIC FIELD INTENSITY IN 10' SECTION AT 4139.6 MHz
(COLD TEST, HORIZONTAL EXCITATION THROUGH COUPLER)

FIG. 14

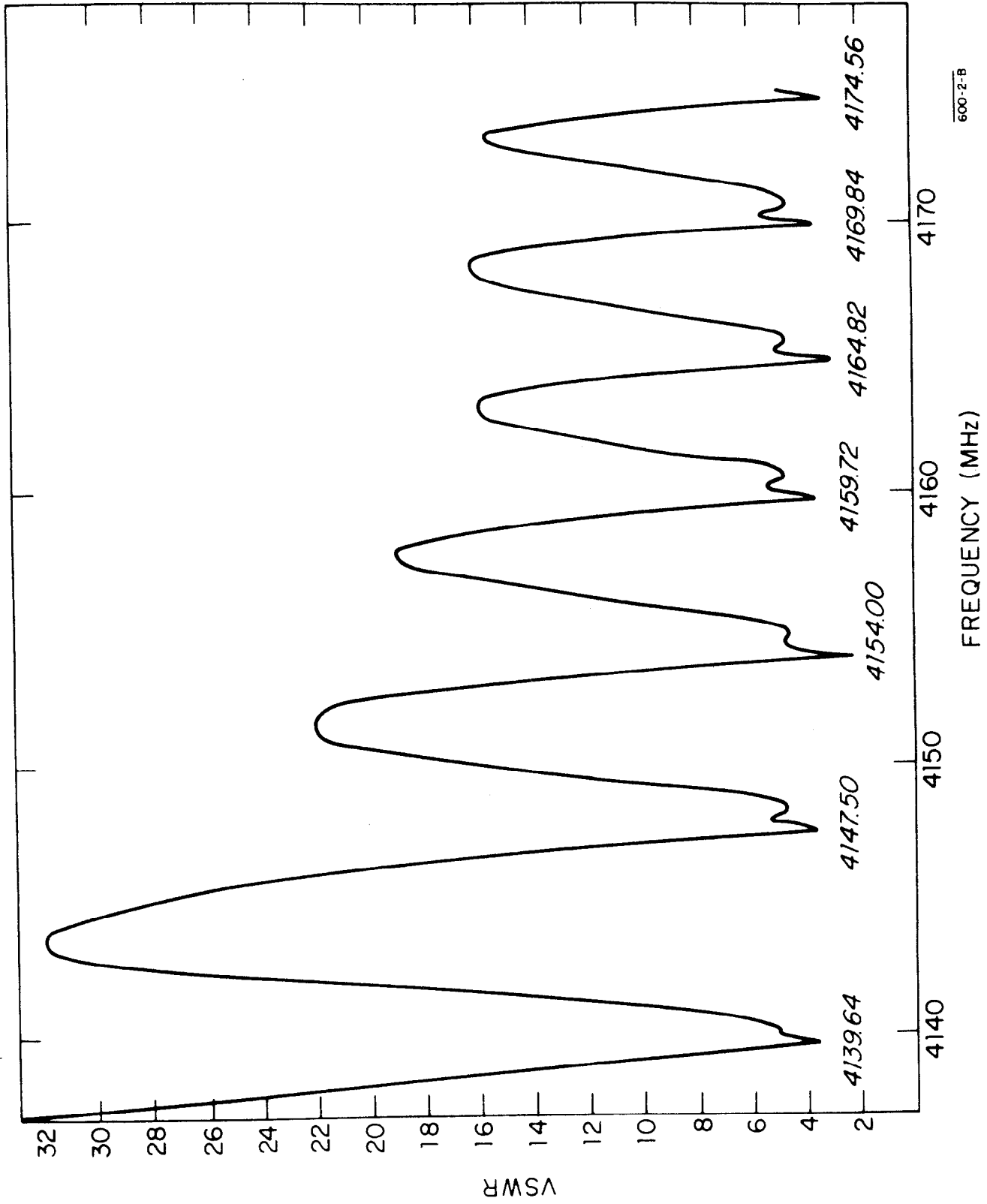


FIG. 15 -- VSWR LOOKING INTO INPUT OF TEN-FOOT ACCELERATOR SECTION

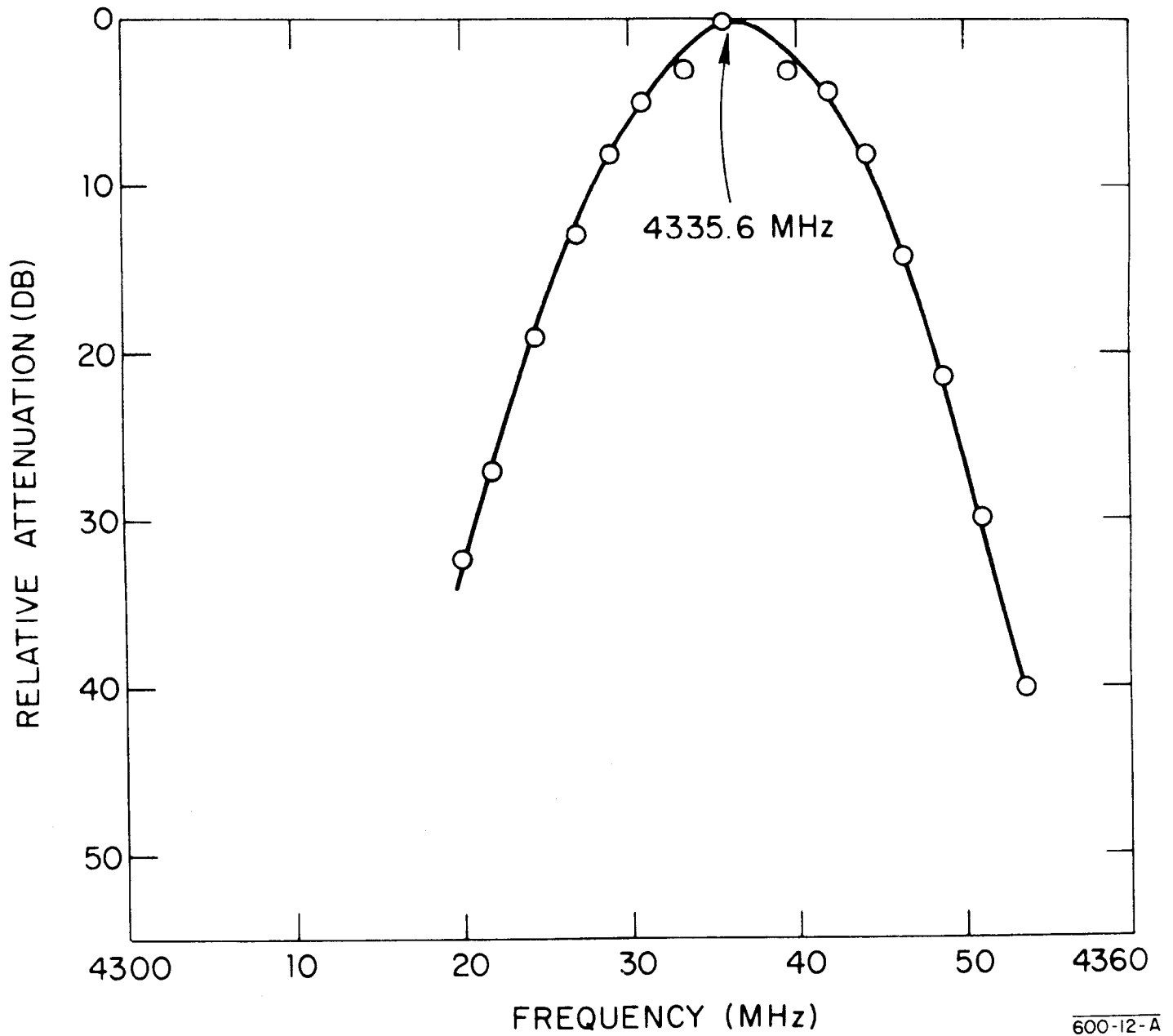
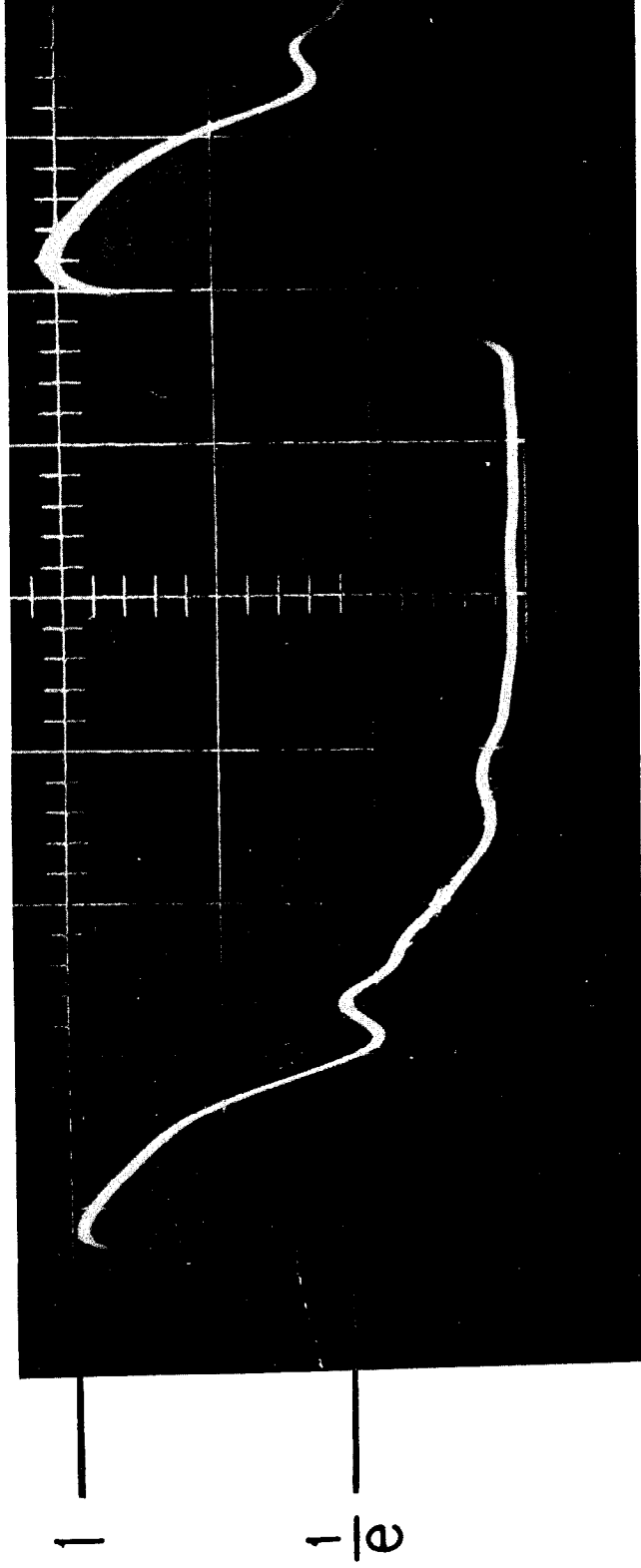


FIG. 16--PASSBAND OF TEN-FOOT CONSTANT-GRADIENT SECTION FOR TM_{11} MODE

$Q_0 \sim 6800$

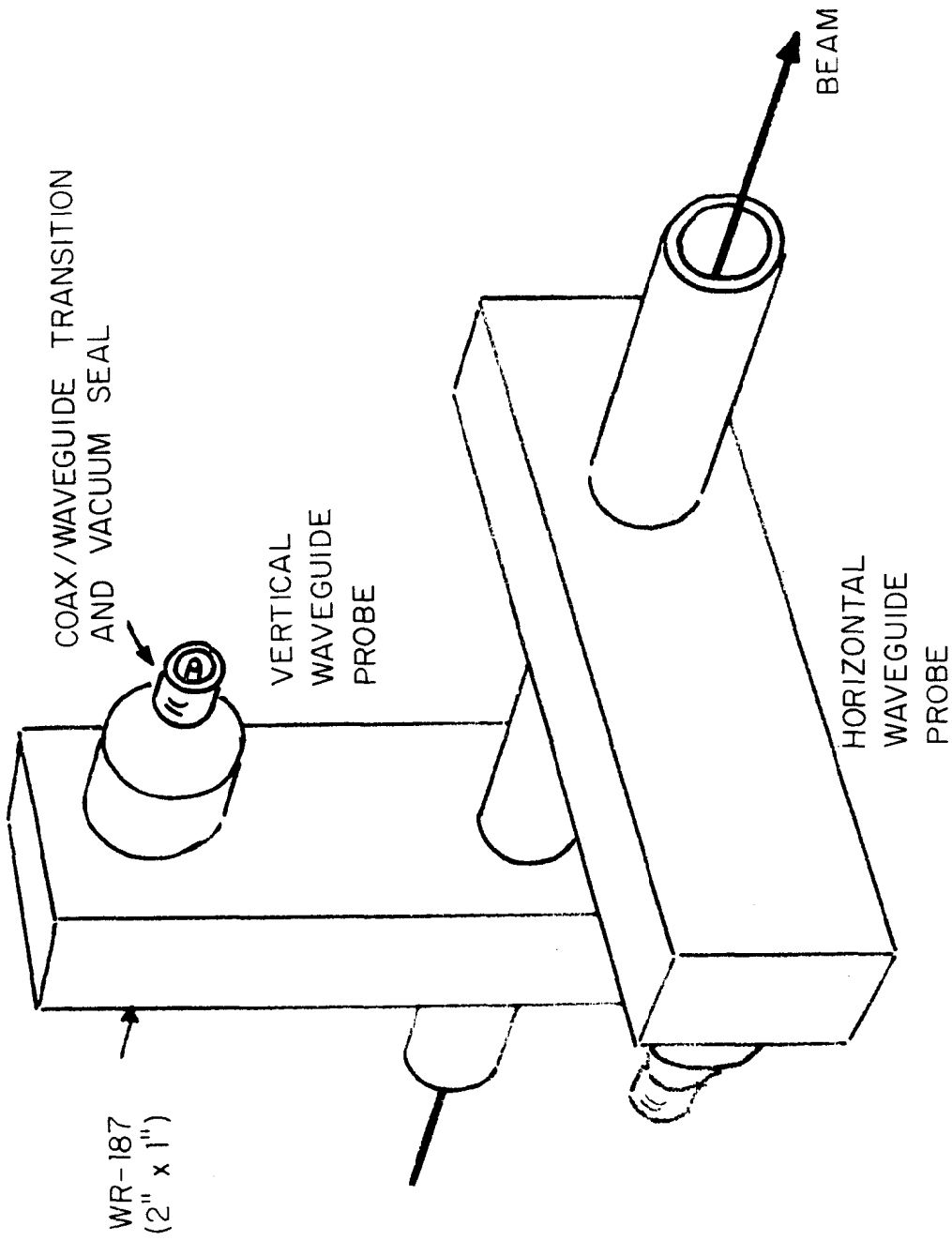


60022A

—|0.13 μs|—

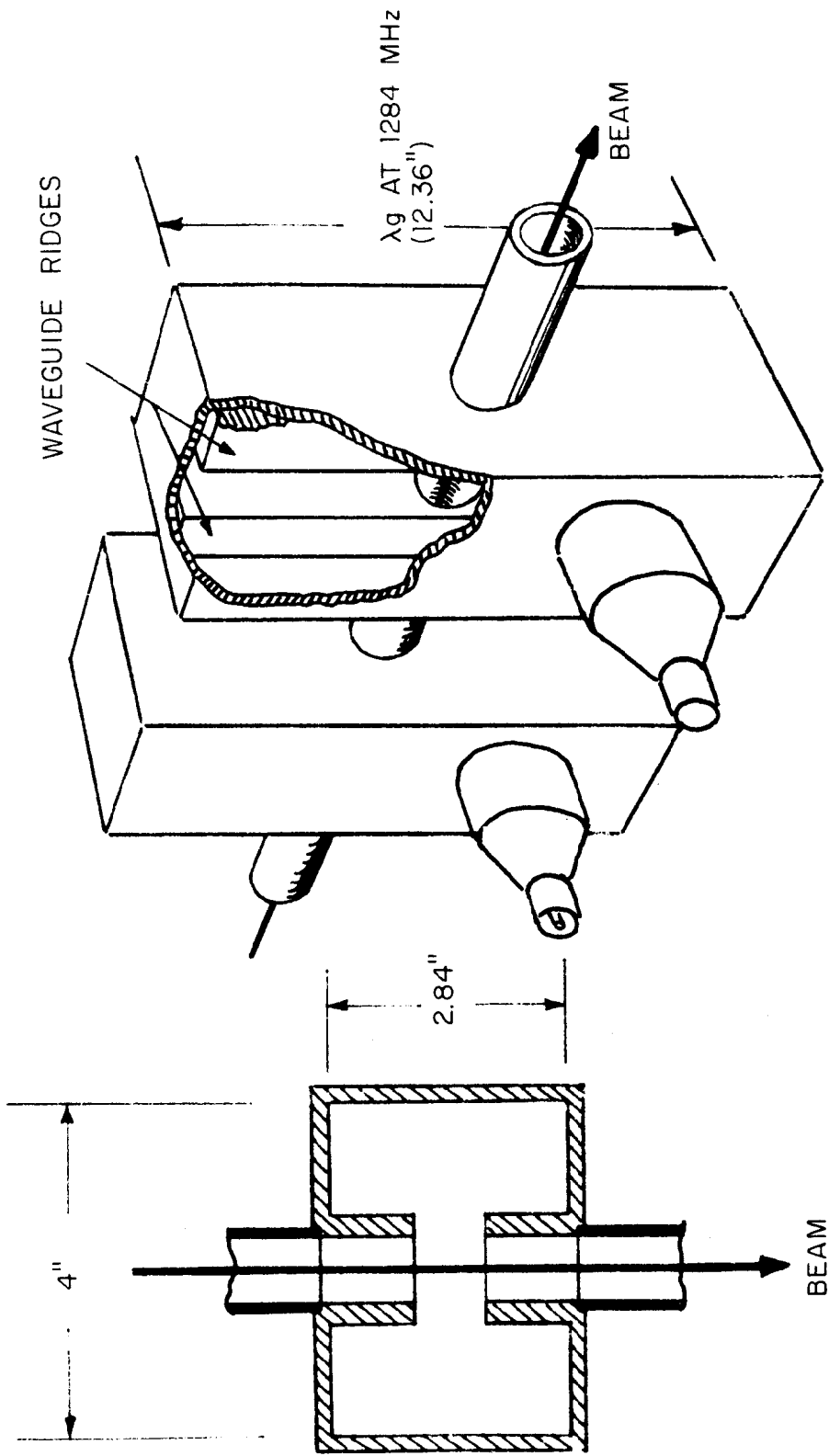
MEASUREMENT OF Q AT 4139.6 MHz BY RINGING
TECHNIQUE (MATCHED CASE, $Q_L = \frac{Q_0}{2}$)

FIG. 17



600-13-A

FIG. 18 -- 4140 MHz CAVITIES USED IN BBU EXPERIMENTS
BOTH CAVITIES ARE 7.9" LONG



TWIN RIDGED WAVEGUIDE CAVITIES

HORIZONTAL SECTION

600-10-A

FIG. 19--1284 MHz CAVITIES USED IN BBU EXPERIMENTS

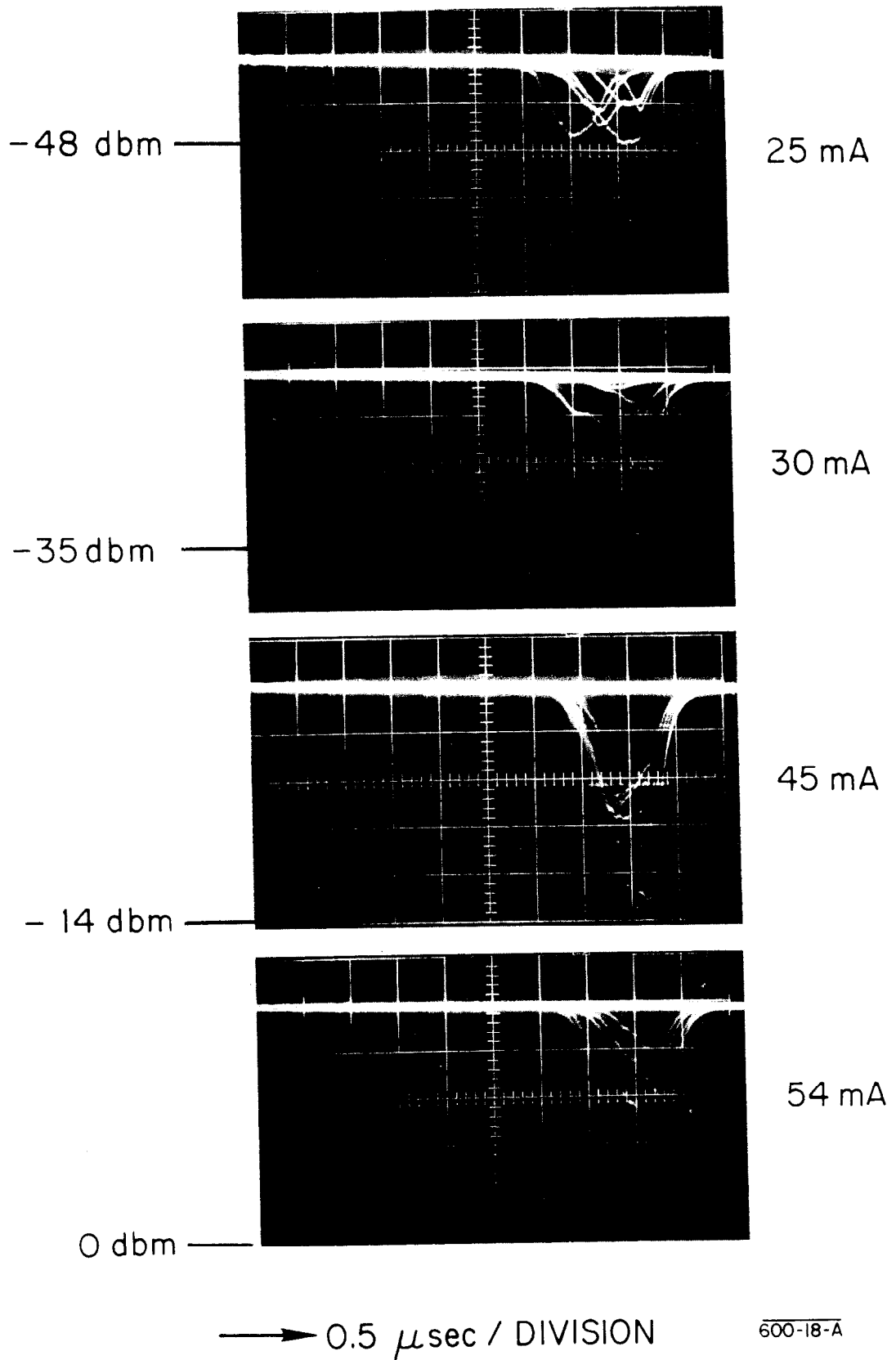


FIG. 20--RF PULSES INDUCED AT 1284 MHz IN
 SECTOR 3 CAVITIES (ENERGY ~1 GeV)

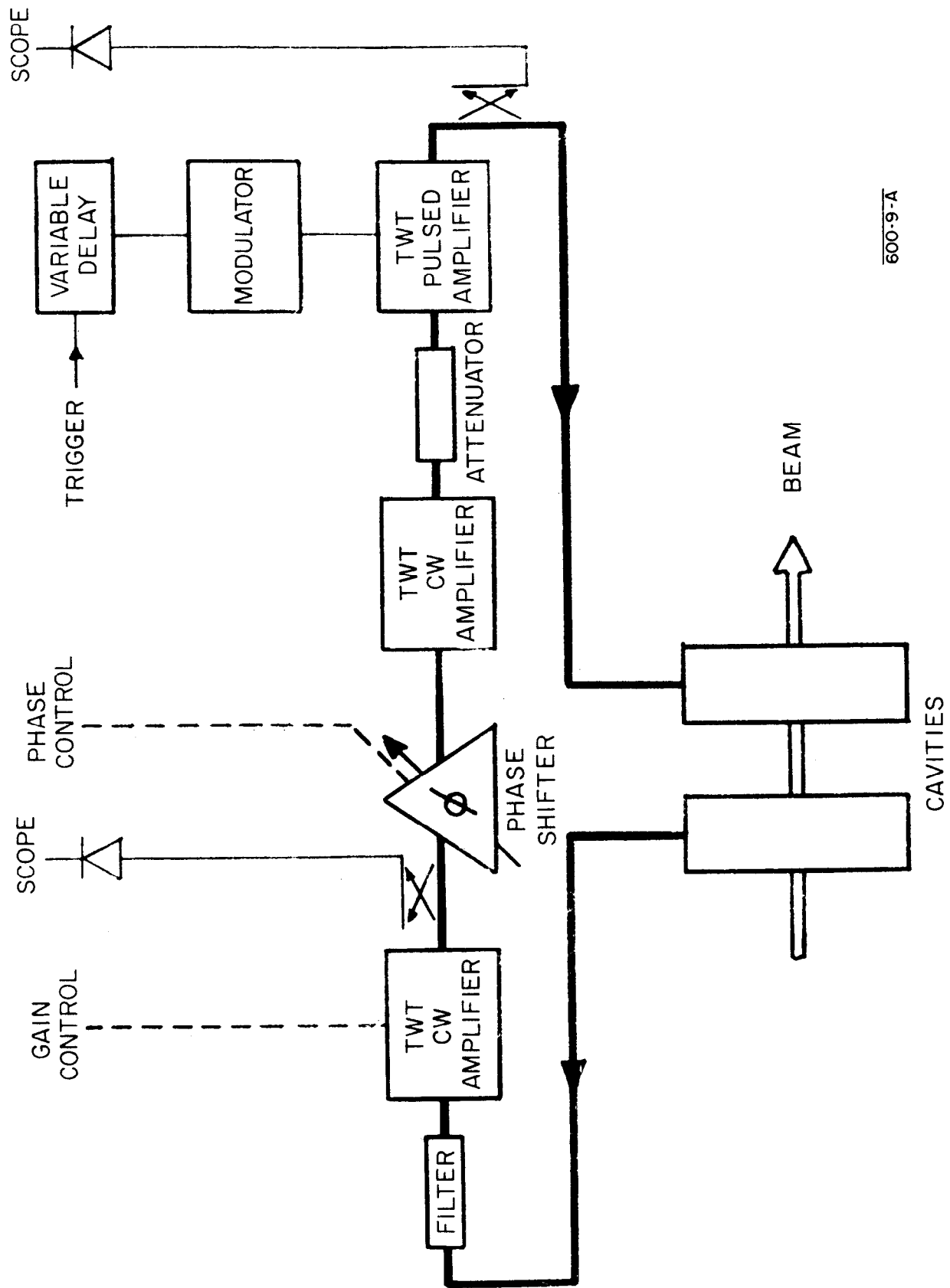
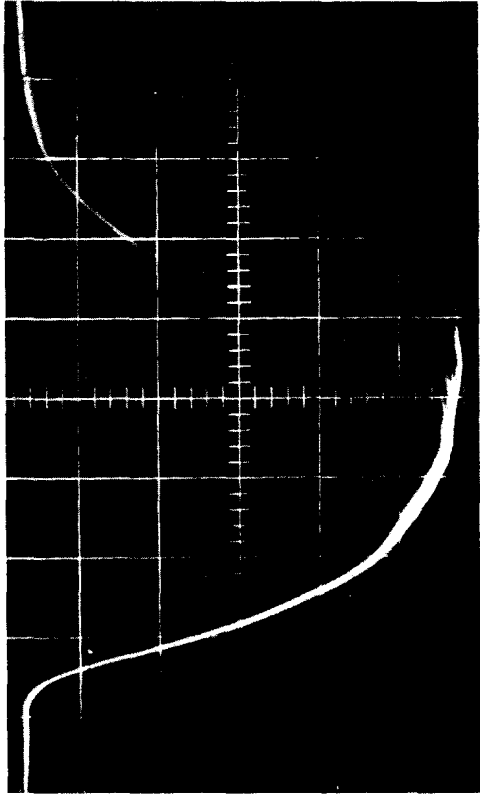
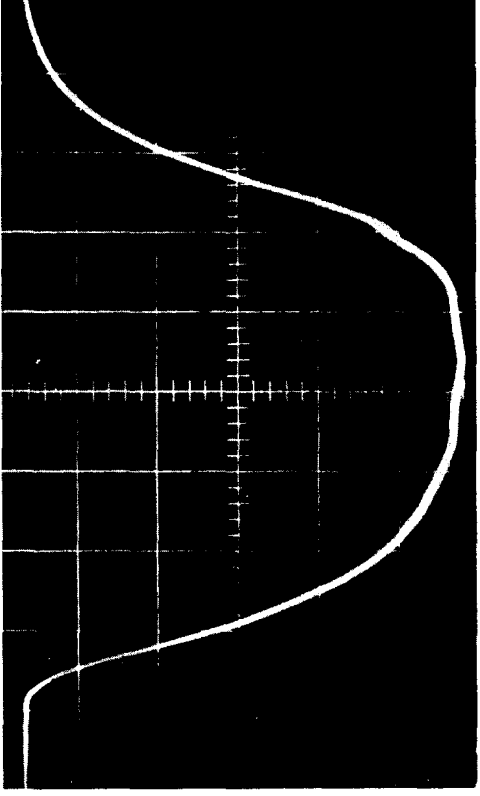


FIG. 21 -- BEAM BREAK-UP FEEDBACK EXPERIMENT



PULSE-SHORTENING AT THE END OF SECTOR
6 DUE TO BEAM BREAK-UP



ELIMINATION OF PULSE-SHORTENING
BY FEEDBACK AT SECTOR 3

CURRENT AT SECTOR 3 = 38 mA

600-7-A

FIG. 22--EFFECT OF FEEDBACK AT 1284 MHZ

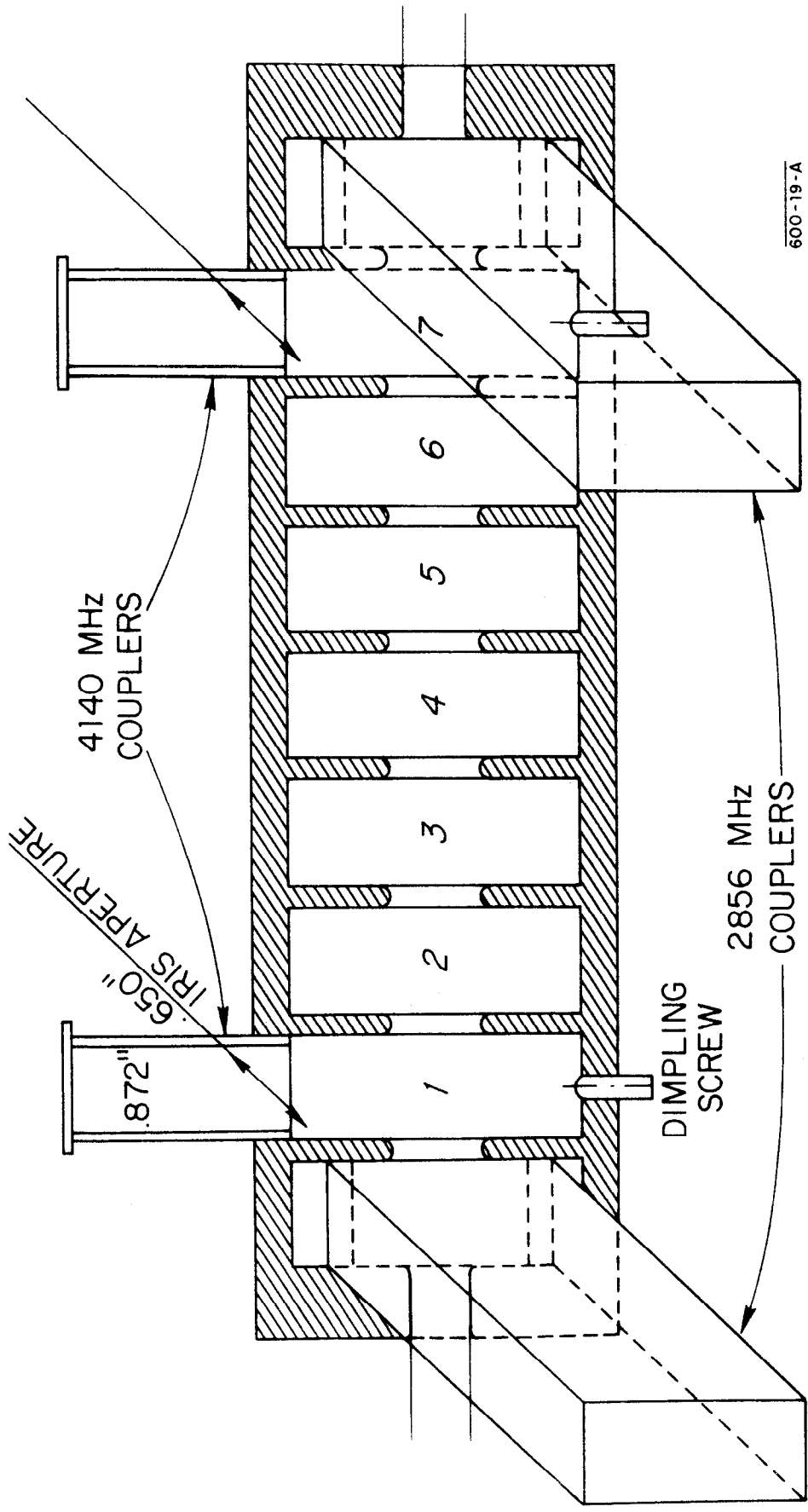
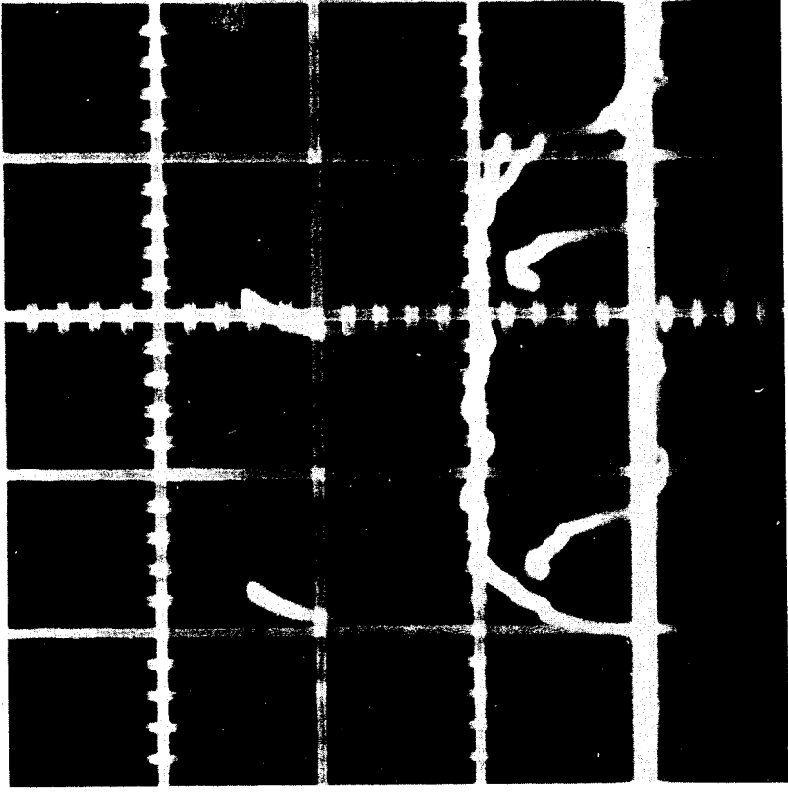


FIG. 23--CONSTANT-GRADIENT INPUT SUBASSEMBLY WITH BOTH 2856 AND 4140 MHz COUPLERS



0.5 μ sec / DIVISION

FIG. 24--EXAMPLE OF TWO INTERLACED BEAMS,
ONE OF WHICH CONSISTS OF TWO SHORT
(~ 150 nsec) SUB - PULSES 60028A

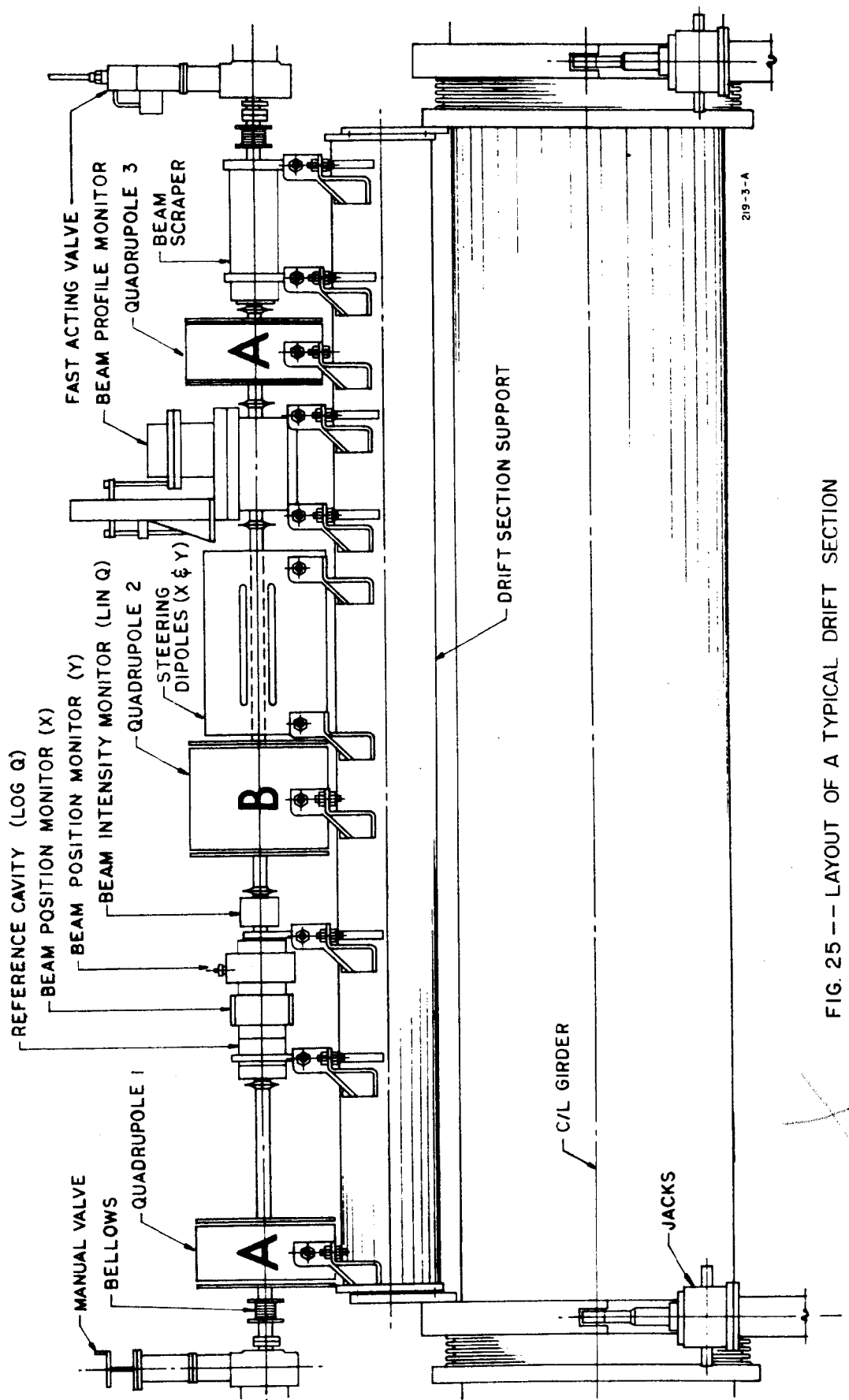
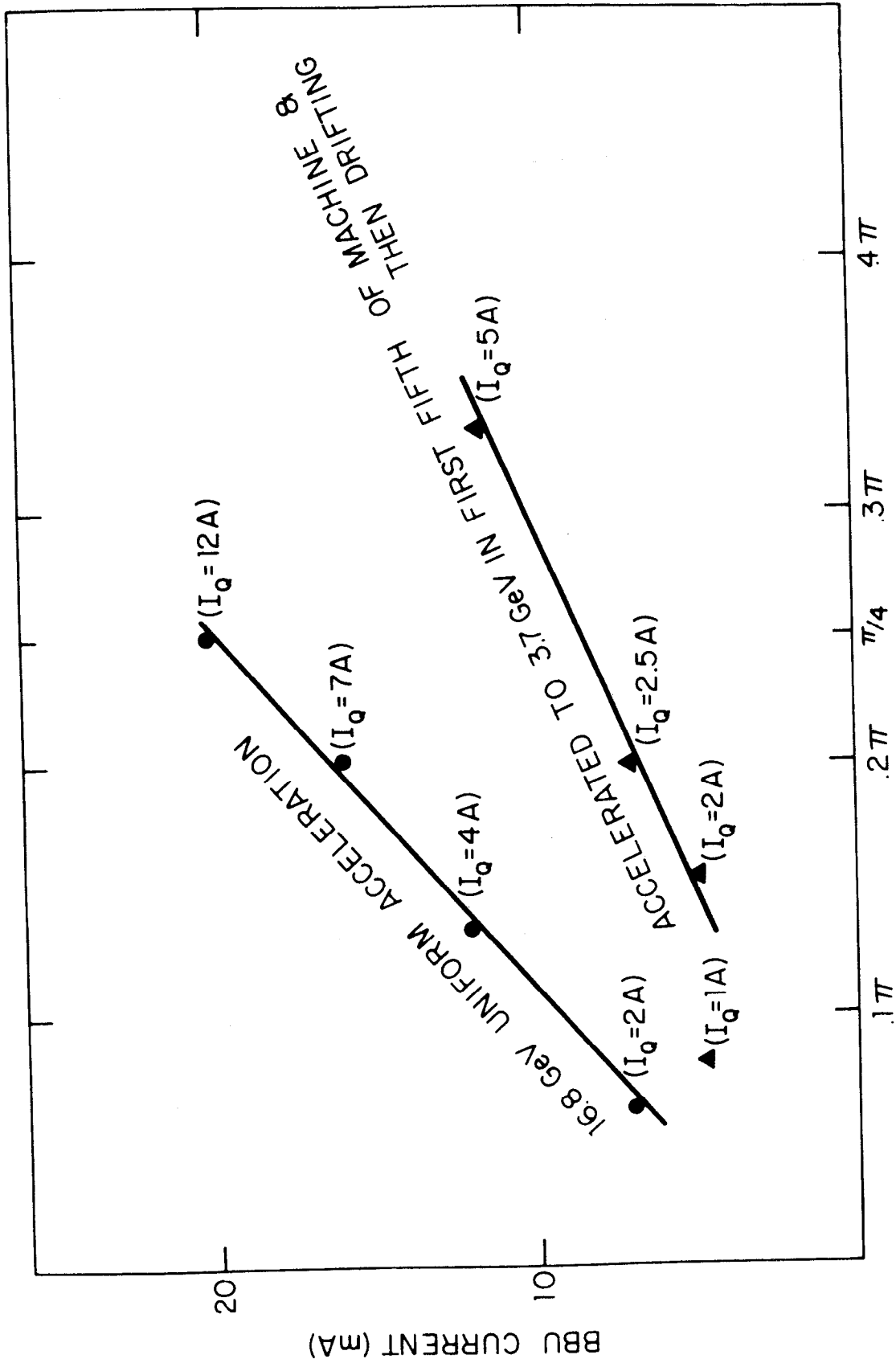


FIG. 25 -- LAYOUT OF A TYPICAL DRIFT SECTION

167 m35 - 21

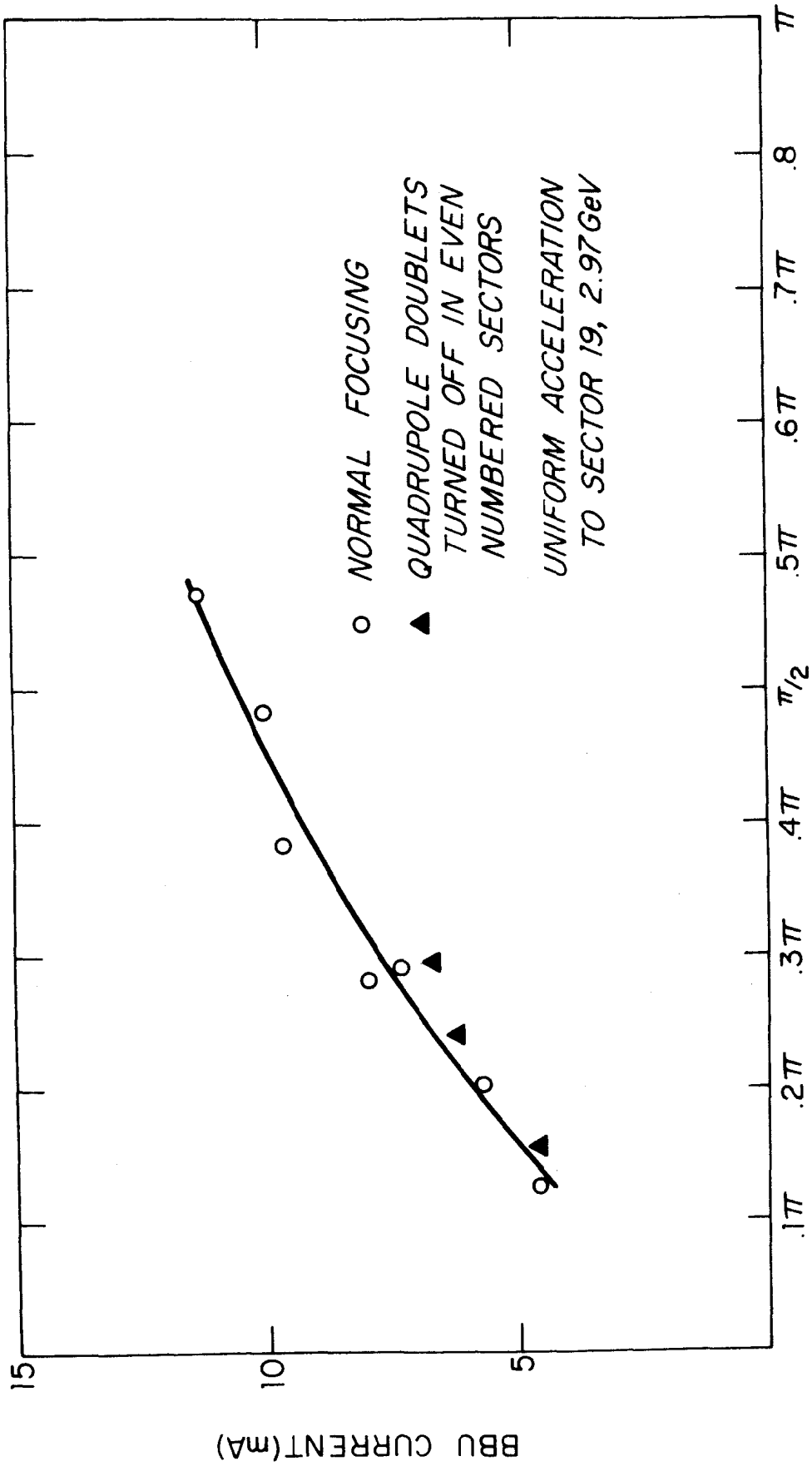


BETATRON PHASE SHIFT PER SECTOR

600-20-B

FIG. 26--BBU CURRENT vs FOCUSING

167 m35-3



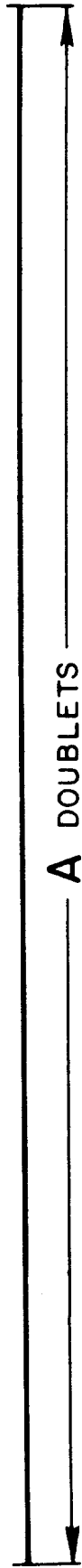
600-29-B

BETATRON PHASE SHIFT PER SECTOR

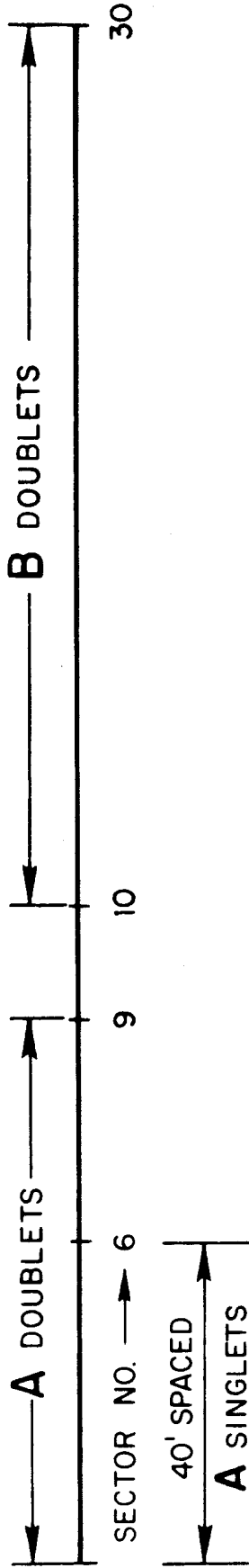
FIG. 27--BBU CURRENT vs BETATRON PHASE SHIFT PER SECTOR

X

PRESENT



FUTURE



600 24A

FIG. 28--PRESENT AND FUTURE QUADRUPOLE DEPLOYMENT

167 M35-2

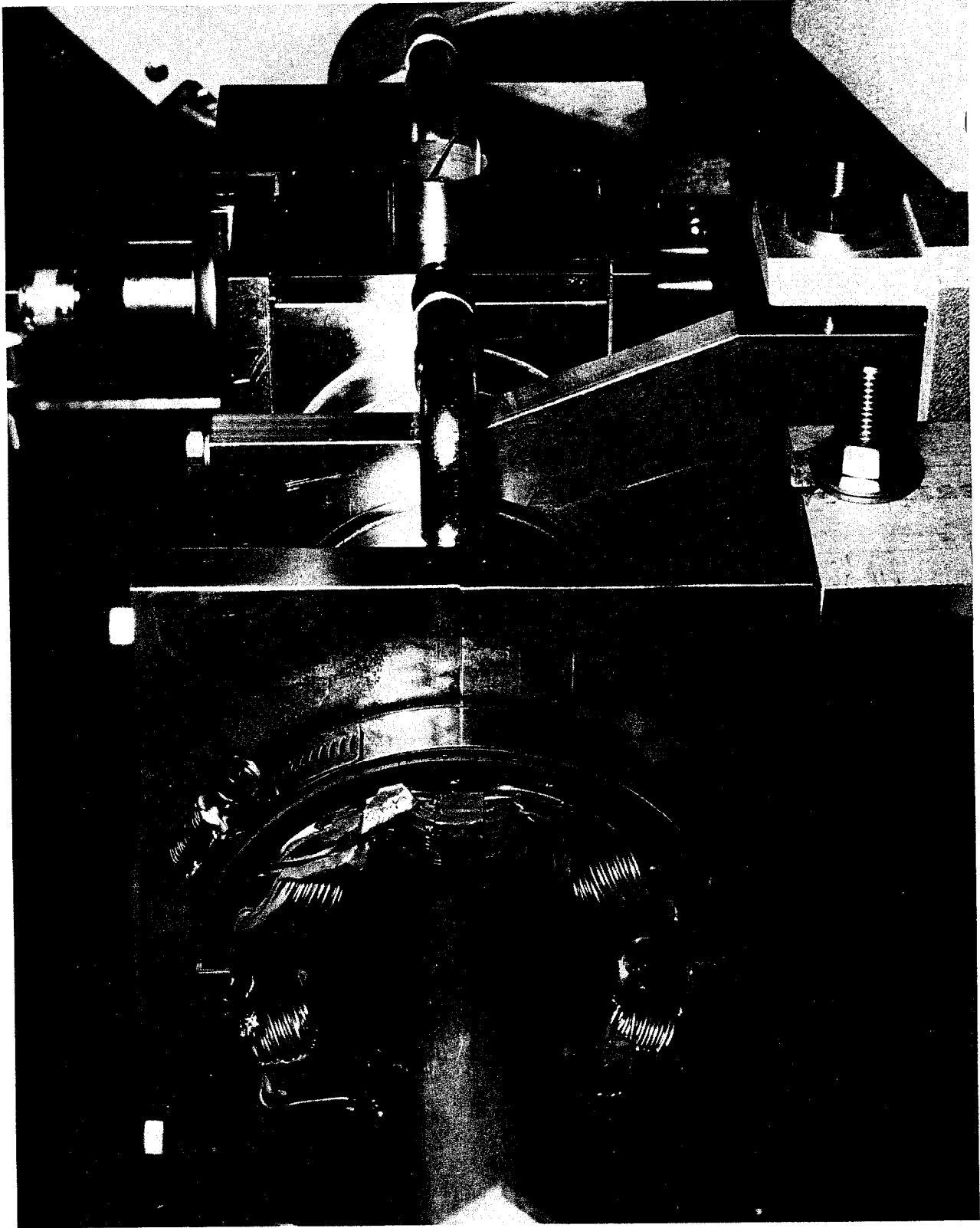


Fig. 29---\$12.00 sextupole magnet.



THE BEAM GETS TO SECTOR 1



THE BEAM IS STUCK IN SECTOR 11



THE BEAM APPEARS IN SECTOR 13



THE BEAM HITS SECTOR 20!

FIG. 30

M. J. 13-73